Received: 13 November 2024 | Accepted: 22 April 2025

DOI: 10.1002/csc2.70089

Crop Science

ISSUES

Special Section: 15th International Symposium on Pre-Harvest Sprouting in Cereals

Identification of LMA-tolerance QTL in a biparental winter wheat mapping population (Xerpha/Bobtail)

Elliott J. Marston[1] | **Marcus A. Hooker**[1] | **Karol Marlowe**[2] | **Travis R. Ruff**[2] | **Yan Liu**[2] | **Scott W. Carle**[3] | **Rehana S. Parveen**[3] | **Susanne Trittinger**[4] | **Deven R. See**[1,2] | **Camille M. Steber**[2,3]

[1]Department of Plant Pathology, Washington State University, Pullman, Washington, USA

[2]USDA-ARS, Wheat, Health, Genetics, and Quality Unit, Pullman, Washington, USA

[3]Department of Crop and Soil Science, Washington State University, Pullman, Washington, USA

[4]Department of Crop and Soil Science, Oregon State University, Corvallis, Oregon, USA

Correspondence
Elliott J. Marston, Department of Plant Pathology, Washington State University, Pullman, WA, USA.
Email: elliott.j.marston@wsu.edu;
Camille M. Steber, USDA-ARS, Wheat, Health, Genetics, and Quality Unit, Pullman, WA 99164, USA.
Email: camille.steber@usda.gov

Assigned to Associate Editor Sivakumar Sukumaran.

Funding information
U.S. Department of Agriculture-Agricultural Research Service

Abstract

Late-maturity α-amylase (LMA) is an emerging cause of low falling numbers in US wheat (*Triticum aestivum* L.) causing financial losses for growers. Quantitative trait loci (QTLs) associated with α-amylase expression during mid-late grain fill, characteristic of LMA, have been mapped across all three wheat genomes. To facilitate breeding for tolerance in soft white winter wheat, QTLs were mapped in a recombinant inbred line population derived from a cross between LMA-susceptible Xerpha and LMA-tolerant Bobtail. The population was characterized for kernel α-amylase activity with cool-temperature LMA-induction (*Lind*) and without (*Lcon*) in field plots from 2019 to 2021. Broad-sense heritability (H^2) was estimated at 0.81 and 0.66 for untreated and induced replicates, respectively, suggesting a genetically inherited trait. A novel major QTL, *QLind-wsu-7A.2*, was mapped to chromosome 7AS and contributed up to 15% of the total phenotypic variation for α-amylase activity in LMA-induced material. Five additional QTLs associated with α-amylase activity after LMA induction, and four QTLs associated with lower α-amylase level in untreated controls, were identified on chromosomes 2A, 3A, 3B, 5B, 6B, 7A, and 7D. All QTLs associated with higher α-amylase levels in untreated material carried

---

Abbreviations: BLUP, best linear unbiased predictor; CIM, composite interval mapping; FN, falling number; GA, gibberellin A; GBS, genotyping-by-sequencing; Lcon, LMA constiutive; Lind, LMA induced; LMA, late-maturity α-amylase; MAS, marker-assisted selection; MLM, mixed linear model; PHS, preharvest sprouting; PNW, Pacific Northwest; QTL, quantitative trait locus; REML, restricted maximum likelihood; RH, relative humidity; *Rht*, reduced height; RIL, recombinant inbred line; SNP, single nucleotide polymorphism; SSR, simple sequence repeat; *wt*, wild-type.

Deven R. See and Camille M. Steber contributed equally to this work.

the Xerpha allele, and most QTLs associated with lower α-amylase levels following cool-induction carried the Bobtail allele. The *Rht-B1b* (where *Rht* is reduced height) and *Rht-D1b* gibberellin A-insensitive semidwarf alleles, known to be associated with LMA tolerance, reduced α-amylase levels in untreated material. Interestingly, the *Rht-B1b/Rht-D1b* double dwarfs consistently expressed higher α-amylase levels with LMA induction, suggesting a complex role for GA signaling in LMA.

Plain Language Summary

Farmers suffer serious losses if their wheat grain contains elevated levels of the enzyme α-amylase because it poses a risk to baked product quality. Late-maturity α-amylase (LMA) is the expression of α-amylase enzyme during late grain maturation, a time when α-amylase levels should be decreasing. LMA is induced by cool temperature shock in susceptible varieties during the soft dough developmental stage. This study found that a more extreme temperature drop gave stronger LMA induction. We mapped the first genes/loci for LMA tolerance in soft white winter wheat, a popular market class in the US Pacific Northwest that has struggled with LMA. We mapped a novel major gene on wheat chromosome 7AS called *QLind-wsu-7A.2* but did not map the major 7B QTL *LMA-1* previously found in spring wheat. This should decrease financial risk for wheat farmers in temperate regions by providing new genes for selection of LMA tolerance in winter wheat breeding programs.

1 | INTRODUCTION

Late-maturity α-amylase (LMA) in allohexaploid wheat (*Triticum aestivum* L.) is an emerging issue causing economic losses for growers worldwide including the US Pacific Northwest (PNW) (reviewed by Cannon et al. [2022] and D. J. Mares and Mrva [2014]). A complex trait influenced by an individual's genotype, developmental stage, and growth environment, LMA is characterized by expression of α-amylase when cool growth conditions occur during the maturation phase of grain development (reviewed in Cannon et al. [2022]). Preharvest sprouting (PHS) is the initiation of mature grain germination on the mother plant, including the mobilization of starch by α-amylase, in response to rain before harvest. The two leading sources of high post-harvest wheat α-amylase, PHS and LMA, cause poor end-use quality in wheat products. While many studies have mapped quantitative trait loci (QTLs) for PHS tolerance, relatively few studies have mapped loci for LMA tolerance in spring wheat and none have mapped this trait in winter wheat (reviewed in Cannon et al. [2022] and D. Mares and Mrva [2008]).

Elevated grain α-amylase poses a risk to wheat end-product quality because starch digestion by α-amylase reduces its gelling capacity, resulting in cakes that fall and sticky bread or noodles (reviewed in Fu et al. [2014], D. J. Mares and Mrva [2014], and Olaerts and Courtin [2018]). This risk is detected in the wheat industry using the Hagberg–Perten Falling Number (FN) method originally developed to detect PHS-damaged grain (reviewed by Ross and Bettge [2009]). The FN method measures α-amylase activity based on the time it takes in seconds for a stirrer to fall through a heated flour/water mixture (Hagberg, 1960, 1961; Perten, 1964). More α-amylase digestion of starch reduces the viscosity of the mixture, causing the stirrer to fall faster and produces a lower FN (reviewed by Hu et al. [2022]). US farmers receive a substantial discount for wheat with an FN below the receival stand of 300 s. A low FN usually indicates starch degradation by elevated α-amylase activity, although low protein levels or the high amylopectin to amylose ratio in "waxy" wheat grain can also depress FN (Ross et al., 2012; Zeng et al., 1997). In 2016, Washington State wheat growers lost an estimated $130 million due to LMA-attributed FN discounts (Steber, 2022). Thus, breeding for LMA tolerance is needed to obtain stable FNs in this region.

While LMA and PHS may involve some of the same hormones, genes, and biochemical pathways, dormancy and PHS tolerance are not always well correlated with LMA tolerance (Barrero et al., 2020; Gale et al., 1983; D. J. Mares & Gale, 1990; Mrva & Mares, 2001b, 2001c; Peery et al., 2023). The plant hormone gibberellin A (GA) is known to stimulate α-amylase expression during cereal grain germination and has been implicated in stimulating α-amylase expression during LMA (Barrero et al., 2013; A. Derkx et al., 2021; Farrell et al., 2013; Kondhare et al., 2015; Mrva et al., 2006). The germinating embryo sends the GA hormone signal that triggers α-amylase expression and secretion in the aleurone cell layer surrounding the endosperm; PHS results in a gradient of α-amylase expression with higher expression levels at the embryo proximal end of the kernel. In contrast, LMA results in a more random distribution of α-amylase throughout the aleurone layer (Mrva & Mares, 1996a; Mrva et al., 2006). LMA involves the expression of α-amylase enzyme encoded by the *Triticum aestivum α-amylase1* (*TaAmy1*) and possibly *4* (*TaAmy4*) gene families during the maturation phase of grain development (Barrero et al., 2013; Cheng et al., 2014; Mieog et al., 2017). Expression of *TaAmy1* and *2* is associated with PHS during mature grain germination (Barrero et al., 2013; D. J. Mares & Mrva, 1993). Finally, LMA may have a milder effect on some aspects of end-use quality than PHS, possibly because PHS induces a broader spectrum of hydrolytic enzymes (Fairlie et al., 2022; Kiszonas et al., 2018; Neoh et al., 2021; Newberry et al., 2018; Ral et al., 2018).

In higher plants, GA stimulates seed germination, the transition to flowering, and stem and leaf elongation by triggering the ubiquitin-mediated proteolysis of the DELLA (Asp-Glu-Leu-Leu-Ala) domain repressors of these GA-stimulated processes (Hauvermale et al., 2012; Hirano et al., 2008; McGinnis et al., 2003). The DELLA genes of wheat are the *reduced height-1* loci, *Rht-A1*, *Rht-B1*, and *Rht-D1* (Pearce et al., 2011; Peng et al., 1999). Deletion of or mutations in the N-terminal DELLA regulatory domain result in a protein that is resistant to GA-targeted destruction, resulting in a GA-insensitive gain-of-function dwarf phenotype. The semidominant semidwarf *Rht-B1b* and *Rht-D1b* alleles of wheat are examples of such DELLA domain mutations resulting from a truncated N-terminal DELLA regulatory domain (Pearce et al., 2011; Peng et al., 1999; Y. Zhang et al., 2021). These alleles have been incorporated into most wheat varieties since the Green Revolution of the 1940s because the semidwarf stature increases yield through resistance to lodging and the partitioning of more resources to grain production (Allen, 1986; Gale & Youssefian, 1975; Youssefian et al., 1992).

Mutations affecting GA hormone signaling have a strong influence on LMA phenotypes (Farrell et al., 2013; Kondhare et al., 2013; D. Mares et al., 2022). In addition to dwarfism, the GA-insensitive *Rht-B1b* and *Rht-D1b* alleles are associated with increased PHS and LMA tolerance (Börner et al., 2018; Fairlie et al., 2024; Farrell et al., 2013; D. J. Mares & Mrva, 2014; D. Mares et al., 2024; Mohler et al., 2014). In some but not all backgrounds, the wild-type (*wt*) tall *Rht-B1a/Rht-D1a* genotype results in a constitutive LMA phenotype where α-amylase is expressed during mid-late grain development without requiring a cold temperature shock (Farrell et al., 2013; Liu, Parveen et al., 2021). The currently accepted model is that GA-insensitivity due to semidwarfing alleles *Rht-B1b* and *Rht-D1b* suppresses constitutive LMA expression resulting in a requirement for cold induction of α-amylase during the soft dough stage of grain development (A. P. Derkx & Mares, 2020; Liu, Tuttle et al., 2021; D. Mares et al., 2022; Mrva & Mares, 1996b, 2001b; Mrva et al., 2009; Tan et al., 2010). Dwarfism alone does not confer a cold-inducible LMA phenotype since the *Rht8*, *Rht13*, and *Rht18* dwarves that are not GA-rescued or GA-insensitive appear to have no effect on LMA phenotype (Fairlie et al., 2024; D. Mares & Mrva, 2008). The 1BL/1RS translocation from rye results in a cold-independent constitutive LMA phenotype even in the presence of *Rht-B1b* or *Rht-D1b* dwarfing alleles, suggesting that this phenotype is not always DELLA-repressed (Farrell et al., 2013; Kondhare et al., 2013; Mohler et al., 2014; Mrva et al., 2009). The inconsistency of the combined effect of temperature and GA sensitivity has led some researchers to suggest that both DELLA-dependent and DELLA-independent mechanisms contribute to LMA tolerance and total levels of α-amylase accumulation during grain filling (Barrero et al., 2013; Liu, Parveen et al., 2021; D. Mares et al., 2022).

Core Ideas

- A major novel quantitative trait locus (QTL) associated with LMA tolerance in winter wheat was mapped to chromosome 7A.
- Seven QTLs associated with late-maturity α-amylase (LMA) tolerance during cold induction were mapped to chromosomes 3B, 5B, 6B, 7A, and 7D.
- Three QTLs associated with high α-amylase activity in untreated controls were mapped to 2A, 3A, and 3B.
- *Rht-B1b* and *Rht-D1b* fail to suppress LMA in cold-shocked double-dwarf lines, indicating complex regulation by Gibberellin A.

Although much remains to be learned about the genetic mechanisms behind LMA, previous studies suggest that multiple loci contribute to the LMA phenotype, though effects are variable and may differ between environments (reviewed in Cannon et al. [2022], D. J. Mares and Mrva [2014], and Mares et al. [2023]). Thus far, a candidate gene has been identified for only one major LMA-associated QTL, the *LMA-1* locus on chromosome 7B (Derkx et al. [2021]). While initial research on LMA in hexaploid wheat focused on Australian germplasm, subsequent work characterized LMA in germplasm from Africa, Asia, Europe, and North America (reviewed in Cannon et al. [2022]). An association study identified LMA-associated QTL on 1A, 3B, 6B, 7A, 7B, and 7D in US and Canadian spring wheat (Liu, Parveen et al., 2021). The QTL on 7B colocalized with the previously cloned *LMA-1* locus. However, winter wheat was strongly impacted by a recent LMA weather event in the US

PNW (Steber et al., 2018). This study characterized LMA tolerance in a soft white winter wheat recombinant inbred line (RIL) population and identified LMA-associated QTL controlling α-amylase expression under both normal and cold-treated conditions. Screening for LMA susceptibility can be a time and labor-intensive process; QTL detection represents the initial phase toward identifying and developing LMA-linked markers for use in marker-assisted selection (MAS) and efficient selection for LMA tolerance by wheat breeders. Releasing LMA-tolerant lines is the most effective way to protect growers from potential financial hardship.

2 | MATERIALS AND METHODS

2.1 | Germplasm

The RIL population of 178 lines was derived by single plant descent of self-pollinated flowers to the F_5:F_6 generation from a cross between LMA-susceptible Xerpha (Eltan/Estica) and LMA-tolerant Bobtail (Einstein/Tubbs) at Oregon State University (Dobrotvorskiy et al., 2023; Jones et al., 2010; Zemetra et al., 2013). Xerpha was characterized as LMA susceptible and Bobtail as moderately tolerant based on FN from natural field LMA events in 2013, 2014, and 2016 (Sjoberg et al., 2020). These LMA phenotypes were confirmed by greenhouse and field LMA induction experiments performed in 2017 and 2018 using methods described by Liu, Parveen et al. (2021) and Liu, Tuttle et al. (2021). Xerpha and Bobtail are soft white winter lines carrying the *Rht-B1b* and *Rht-D1b* semidwarfing alleles, respectively. The F_5 RIL population and parents were grown as double headrows at the Spillman Agronomy Farm in Pullman, WA, in 2019, and F_6 seed from single plants was used to plant headrows in 2020 and 2021. These experiments were planted on October 12, 2018; September 27, 2019; and October 20, 2020, respectively. When planted in 2019, headrows of mixed awn type were observed (Table S1). If a line showed a mixed awn type, only awnless heads were advanced due to the recessive nature of the trait. One more generation of single-spike descent was performed in the 2020 field season to decrease segregation, and the resulting progeny were used to plant in 2021. The population was scored for awn type again in 2020 to verify consistency within lines. Final plant height was recorded in centimeters during the 2020 field season after lines had matured. Seven RILs that displayed a mixed awn type in 2019 were excluded from the final data analysis.

2.2 | Field LMA phenotyping

A detached-tiller method was used to induce LMA in field-grown material as described in Liu, Parveen et al. (2021) and Liu, Tuttle et al. (2021). Two randomized complete blocks of 178 RILs plus the parents from the Xerpha/Bobtail mapping population were LMA treated in 2019 and 2020, plus one complete block in 2021. The anthesis date for each pair of headrows was recorded based on the date when 50% of all spikes had reached anthesis. Headrows were sampled for LMA induction at 475–520 growing degree days past-anthesis to obtain 15–20 random tillers at the soft-dough stage of grain filling (Zadok growth stage 85), the growth stage when wheat becomes susceptible to LMA induction (A. P. Derkx & Mares, 2020; Liu, Tuttle et al., 2021; Zadoks et al., 1974). Briefly, tillers were cut above the soil line, bundled, and placed immediately stems-down into buckets with water to keep tillers alive, and LMA was induced using a cold treatment of 7 days of 18°C day/7.5°C night, 55%–75% relative humidity (RH), and a 16-h photoperiod. Two LMA-treated replicates were harvested in both 2019 and 2020; only a single LMA-treated replicate was harvested in 2021 (Table 1). After the 7-day cold treatment, the treated spikes were placed outside in buckets of water to finish maturing. The same field headrows sampled for LMA-treatment were sampled directly from the field at harvest maturity as untreated controls: one field replicate in 2019, two in 2020, and one in 2021. Twenty spikes from each headrow were bulked and threshed with a head-thresher. Once threshed, 15–20 g grain samples were milled using a UDY Cyclone Sample Mill with a 5 mm screen (www.udyone.com) before megazyme α-amylase sprout damage (SD) assays (K-AMYLSD) were performed on 0.2 g of meal with a ChemWell-T robot as described in Hauvermale et al. (2023). The absorbance of samples during the SD assay was measured at 405 nm and reported as SD units/g (SDU/g). Ambient air temperature as measured at 1.5 m, RH, and precipitation data for June and July in 2019 to 2021 from the Pullman, WA, AgWeatherNet station were used to measure and assess differences in growing conditions between years

TABLE 1 Summary and overview of experimental replicates.

Replicate name	Year	Treatment type	SDU/g mean and SD[a]
2019.LMA1	2019	LMA-treated	0.33 ± 0.72
2019.LMA2	2019	LMA-treated	0.30 ± 0.56
2019.U1	2019	Untreated/control	0.11 ± 0.06
2020.LMA1	2020	LMA-treated	0.37 ± 0.44
2020.LMA2	2020	LMA-treated	0.46 ± 0.87
2020.U1	2020	Untreated/control	0.11 ± 0.04
2020.U2	2020	Untreated/control	0.12 ± 0.06
2021.LMA1	2021	LMA-treated	1.15 ± 1.34
2021.U1	2021	Untreated/control	0.12 ± 0.04

Abbreviations: LMA, late-maturity α-amylase; SD, standard deviation; SDU, sprout damage units.

[a] Untransformed α-amylase activity (SDU/g) as read at 405 nm.

that might contribute to LMA phenotypes (Table S2; Rasul et al., 2015).

2.3 | Statistical data analysis

R (v4.2) was used to perform multistep data normalizations and comparisons among replications and years. Replicates displayed a Poisson distribution for α-amylase activity, particularly in cold-treated replicates, with values heavily skewed toward low SDU/g values. Fitness and efficiency of Gaussian, square root, cube root, and Log_{10} transformations were compared using the lme4 package (Figure S1; Bates et al., 2014; lme4 v1.1-34). Based on quantile–quantile (Q–Q) plots and Akaike information criterion values, a cube root transformation was selected for normalization of SDU/g data (Figure S2; Butler et al., 2009). No transformation of untreated controls was needed before calculating best linear unbiased predictors (BLUPs). For treated data, BLUPs were calculated across all replications and all years using cube root transformed data; BLUPs were not calculated for single year data. For years, with multiple replicates, average values between replicates were calculated. Average treated and untreated values across replicates for all years were also calculated for each line. The average treated and untreated values within and across years were normalized using an absolute cube root transformation before mapping. Incidence of LMA across all years in treated and untreated control groups was determined for each line using α-amylase activity thresholds of $\geq$0.24 SDU/g or 0.62 for cube root transformed data, which is equivalent to an FN of 250 s (Hauvermale et al., 2023). Incidence of LMA scores in LMA-treated and -untreated replicates was calculated by dividing the number of times a line had an SD value above these thresholds by the total number of LMA-treated or -untreated replicates ($n = 5$ and $n = 4$, respectively). The FN was estimated based on the equation from Hauvermale et al. (2023) where x is FN:

$$\text{SDU/g} = 3.82e^{-0.011x}.$$

Analysis of variance (ANOVA) was performed on absolute cube root transformed SDU/g values in combination with genotype, year, and treatment type as factors using the lme4 package (Table 2; Bates et al., 2014). ANOVA was also used to examine the impact of awn type and *Rht* genotype on phenotypic variance in combination with treatment type and year (Table S3). Phenotypic variance was calculated by dividing the group sum of squares by the ANOVA total sum of squares. Restricted maximum likelihood (REML) was used to fit a mixed linear model (MLM) that was performed separately on the LMA-treated and -untreated data for all years to calculate BLUPs with the lmer function in lme4 with genotype and year as random effects (Tables S4 and S5; Gilmour et al., 1995; Henderson, 1975; lme4 v1.1-34). The resulting variances were used to estimate broad-sense heritability (H^2) using the following equation:

$$H^2 = \frac{V_{\text{genotype}}}{V_{\text{genotype}} + \left(V_{\text{residual}}/\#\ \text{replicates}\right)},$$

where V_{genotype} is the variability associated with genotype, V_{residual} is the residual error in the model, and # replicates is the total number of replicates included in the model. Heritability was calculated for both cold-treated and -untreated control replicates across all years using an MLM with genotype and treatment type as random effects. Year was not included as a factor in these calculations due to the lack of replicates in some years.

2.4 | Genotyping and genotype data analysis

2.4.1 | DNA extraction and GBS library creation

Grain harvested from F_6 plants grown in the 2020 trial headrows was planted in 96-well trays for parental lines and each RIL. Approximately 100 mg of leaf tissue was collected from F_7 plants at the two- to three-leaf stage for each line and then lyophilized for 3 days using a BenchTop Freeze Dryer (SP Scientific). A BioSprint 96 workstation with a BioSprint 96 DNA Plant kit was used to extract and purify total genomic DNA (QIAGEN). Quant-iT PicoGreen dsDNA Assay Kit was used to quantify DNA (Thermo Fisher Scientific) in a Synergy 2 Multi-Mode Reader. An Integra ASSIST PLUS platform was used to normalize DNA to 20 ng/μL and 25 ng/μL for use in genotyping-by-sequencing (GBS) and running simple sequence repeat (SSR) markers, respectively.

PstI and *MspI* restriction enzymes were used to construct GBS libraries using the method of Poland et al. (2012) modified for use in 96-well plates. Once libraries were created, they were assessed for size distribution and quantified using an Agilent High Sensitivity DNA Kit (Agilent Technologies) with an Agilent 2100 Bioanalyzer. Further sequencing steps were completed with the required amount of size-selected GBS library by the North Carolina State University's Genomic Sciences Laboratory using an Illumina NovaSeq 6000 (Illumina Inc.) in September 2021.

2.4.2 | GBS data analysis

Raw sequence data from the NovaSeq 6000 obtained via GBS had individual sample sequences assigned to their respective barcodes and were trimmed to 80 bp from 120 bp. Only sequences that started with a *PstI* site were retained for further

TABLE 2 ANOVA examining sources of variation on α-amylase activity.

Term	df	Sum of squares	Mean of squares	*F*-stat	Pr (> *F*)
Genotype	172	12.40	0.07	5.96	2.69E-56
Year	2	6.07	3.04	251.10	5.79E-77
Treatment	1	20.49	20.49	1694.07	2.05E-165
Genotype:Year	344	11.28	0.03	2.71	4.46E-25
Genotype:Treatment	172	9.29	0.05	4.47	9.91E-40
Year:Treatment	2	5.35	2.67	221.03	3.94E-70
Genotype:Year:Treatment	342	9.40	0.03	2.27	1.46E-17
Residuals	518	6.26	0.01		

Note: Full mixed model with genotype, year, and treatment type and their interactions as random effects.
Abbreviations: ANOVA, analysis of variance.

analysis. This preprocessing was followed by identification of single nucleotide polymorphisms (SNPs) and a sequence homology comparison using the TASSEL (Trait Analysis by aSSociation, Evolution and Linkage) 5 GBS v.2 Pipeline and the International Wheat Genome Sequencing Consortium's (IWGSC) Reference Wheat Genome RefSeq v1.0 (Bradbury et al., 2007; IWGSC, 2018). Both parents in the population had genotype calls generated for both co-dominant and dominant markers if the individual SNPs were present in 20%–80% of the entire population. The software LinkImpute was used to perform SNP imputation after filtering SNPs with thresholds of no more than 80% missing data per SNP and 50% missing data per sample (Money et al., 2015). A total of 3517 SNP markers were identified after imputation of GBS-generated sequence tags by the TASSEL pipeline. Of these markers, 3022 high-quality polymorphic SNPs were retained after filtering SNPs that were missing or heterozygous for parental lines.

2.4.3 | SSR and KASP marker analysis

Parental lines and RILs were assayed for *Rht* alleles of *Rht-B1* and *Rht-D1* with KASP (Kompetitive Allele Specific PCR) markers developed by Ellis et al. (2002). KASP assays were conducted following the standard protocols provided by LGC Genomics (https://www.biosearchtech.com/products/oligos-probes-and-primers/kasp-genotyping-assays/running-kasp-genotyping-reactions). KASP assays were visualized and scored using a LightCycler480 (LC480) (Roche). A total of 948 SSR markers were screened to identify polymorphic markers in the parental lines (Table S6; http://wheat.pw.usda.gov). Forty polymorphic SSR markers were selected to genotype the RILs based on preliminary single marker (SM) analysis that identified chromosomes with potential QTL to verify GBS marker positions. The universal M13 tail (5′-CACGACGTTGTAAAACGAC) was affixed to the 5′ end of each forward primer so polymerase chain reaction (PCR) products could be detected through direct labeling (Schuelke, 2000). One of four fluorescent dyes—FAM (blue), VIC (green), NED (yellow), and PET (red) (Applied Biosystems)—was used to label the M13 universal primers to detect different PCR products. Each 12-μL PCR reaction mix contained 6.48 μL molecular grade H_2O, 1.2 μL Mg-free 10x PCR reaction buffer, 0.4 μL 25 mM $MgCl_2$, 1.2 μL 2.5 mM dNTP, 0.06 μL 10 μM M13-tailed forward primer, 0.3 μL 10 μM reverse primer, 0.24 μL 10 μM M13 labeled with appropriate fluorophore dyes (Applied Biosystems), 0.2 μL of *Taq* DNA polymerase (5 U/μL) (New England Biolabs), and 2 μL template DNA (25 ng/μL). A Biometra TAdvanced thermocycler (Analytik Jena) was used to perform PCR under the following conditions: 94°C for 5 min hot start, 35–41 cycles (depending upon primers) of 94°C for 30 s denaturing, 52°C–61°C (depending upon primers) for 45 s annealing, and 72°C for 1 min, followed by a 10 min final extension at 72°C.

The PCR products, with up to four distinct fluorescent dyes (FAM, VIC, NED, and PET) in amounts of 3, 3, 4, and 6 μL, respectively, were pooled into a single 96-well plate and adjusted to a total volume of 25 μL by adding molecular grade H_2O depending on the number of distinct dyes pooled. From this mixture, 3 μL was transferred to corresponding wells in a new plate. Each well contained a total volume of 13 μL after the addition of 9 μL of highly deionized (Hi-Di) formamide and 1 μL of a 445-bp Cassul DNA ladder (Brownstein et al., 2018). After a 5-min denaturation step at 94°C, the 13 μL mixture underwent capillary electrophoresis using an ABI 3730XL DNA Analyzer (Applied Biosystems). Marker alleles were analyzed and scored using GeneMapper v1.5 software (Softgenetics).

2.5 | Linkage mapping and QTL analysis

Linkage groups were constructed using SNP data generated from the polymorphic GBS tags and SSR data in JoinMap version 4.0 using the regression mapping algorithm (Van Ooijen et al., 2006). The Kosambi mapping function was used to calculate genetic distances (Kosambi, 1943). Markers were assigned to corresponding chromosomes based on the known chromosomal loci of SNP markers based on their alignment with IWGSC RefSeq v1.0 or wheat maps published by Somers et al. (2004) and the GrainGenes database (http://wheat.pw.usda.gov) for GBS tags and SSR markers, respectively (IWGSC, 2018). Linkage groups were constructed using a minimum logarithm of odds (LOD) score threshold of 3.0. Linkage maps were drawn using the LinkageMapView package in R (Ouellette et al., 2018). Relationships between genetic and physical distance for each chromosome linkage group were visualized using the MAST-Script-Suite (Figure S3; Carle, 2020). BLUPs and LMA-incidence scores of the LMA-treated and -untreated control SDU/g values across all years were used to perform a QTL analysis. Individual replicates, replicate averages within years and treatment types, and replicate averages within treatment types but across years were also used to perform QTL analysis for a total of 18 traits (Table S1). QTL analysis was performed in QTL Cartographer v2.5 using both SM analysis and composite interval mapping (CIM) methods. LOD thresholds for QTL detection were set at 3.0 for the SM analysis and then determined separately for each trait using the Selection by Permutation function in QTL Cartographer by conducting 600 permutations with a significance level of 0.05 for the CIM analysis (NCSU, 2010). A forward and backward regression method was used to conduct CIM across all chromosomes and traits.

To approximately compare the positions of QTLs from the current study with those in previous studies, we considered the chromosome arms QTL mapped to, proximity to centromeres, and physical position if reported. QTLs mapped using the untreated samples were designated as LMA-constitutive or "Lcon" QTLs, while QTLs mapped using LMA-treated data were designated as LMA-induced or "Lind" QTLs to distinguish under which growing conditions QTLs were mapped. Phenotype variance explained by the genotype value of specific markers was described using the R^2 value. Minor, moderate, or major QTLs were described as having an R^2 score of $R^2 < 10\%$, $15\% > R^2 > 10\%$, or $R^2 > 15\%$, respectively. The parental allele was described by the effect of individual QTL with negative effects associated with the Bobtail allele and positive effects associated with the Xerpha allele. Putative gene candidates were screened using the annotated IWGSC genome assembly in Ensembl Plants release 57 (IWGSC, 2018; Yates et al., 2022). Full linkage maps and genotype data are available in Table S6.

3 | RESULTS

3.1 | LMA field phenotyping results

Experiments comparing LMA-treated material to untreated material were conducted over three consecutive field seasons (2019–2021) on 173 RILs in the Xerpha/Bobtail biparental mapping population and the parental lines. LMA-treated replicates exhibited elevated α-amylase activity and increased variability compared to untreated replicates within and between all years (Figure 1; Table 1). Significant differences in average values of LMA-treated replicates were observed between years, while average untreated values did not show significant differences (Figure 1; Table 1). The 2019 LMA-treated replicates (2019.LMA1 and 2019.LMA2) showed significantly higher α-amylase expression than untreated controls with an average transformed SDU/g value that fell above the LMA threshold of >0.24 SDU/g, <250 s FN (see Section 2.3) (Figure 1; Table 1). The proportion of samples with sufficient α-amylase activity to give an FN below 250 s rose sharply in 2021 to 93% from 34.4% and 54.2% in 2019 and 2020, respectively. Incidence of LMA in untreated replicates remained below 7.5% for all years. Examination of parental phenotypes revealed that Bobtail maintained a resistant phenotype in all years except the 2021 LMA-treated replicate, whereas Xerpha consistently displayed LMA in LMA-treated samples and higher α-amylase levels than Bobtail in untreated replicates (Figure 2). Raw and cube root transformed SDU/g values for both LMA-treated and -untreated replicates for all years are provided in Table S1.

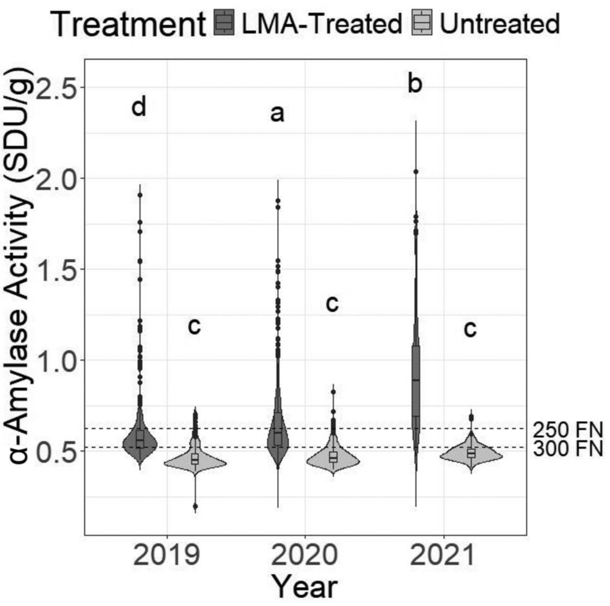

FIGURE 1 Late-maturity α-amylase (LMA) induction across years. LMA-treated (dark gray) and -untreated/control (light gray) sample distribution of cube root transformed α-amylase activity (SDU/g) of the Xerpha/Bobtail mapping population. Similarity of groups is indicated by letters above individually plotted violin plots as calculated by Tukey Honestly Significance Difference test. Five LMA-induced replicates ($n = 865$) and four untreated replicates ($n = 692$) were performed in 2019 ($n = 518$), 2020 ($n = 691$), or 2021 ($n = 345$). FN, falling number; SDU, sprout damage units.

TABLE 3 Correlations and p-values for all cube root transformed and replicate averages.

	Correlation coefficient							
Average replicate	**Average LMA all years**	**Average LMA 2019**	**Average LMA 2020**	**LMA 2021**	**Average U all years**	**U 2019**	**Average U 2020**	**U 2021**
Average LMA all years	1.0	0.565***	0.717***	0.833***	0.163	0.101	0.16	0.145
Average LMA 2019	0.565***	1.0	0.24	0.242	−0.0321	−0.0299	−0.0295	−0.00942
Average LMA 2020	0.717***	0.24**	1.0	0.365***	0.121	0.0575	0.154	0.0587
LMA 2021	0.833***	0.242**	0.365***	1.0	0.223**	0.162	0.189*	0.221
Average U all years	0.163*	−0.0321	0.121	0.223	1.0	0.848***	0.911***	0.625***
U 2019	0.101	−0.0299	0.0575	0.162*	0.848***	1.0	0.642***	0.413***
Average U 2020	0.16*	−0.0295	0.154*	0.189	0.911***	0.642***	1.0	0.391***
U 2021	0.145	−0.00942	0.0587	0.221**	0.625***	0.413***	0.391***	1.0

Note: Individual replicates included if no average can be calculated. Upper half contains adjusted p-values and lower half contains raw p-values.
Abbreviation: LMA, late-maturity α-amylase; U, untreated replicates.
*, **, and ***depict significance at the 0.05, 0.01, and 0.001 probabilities levels.

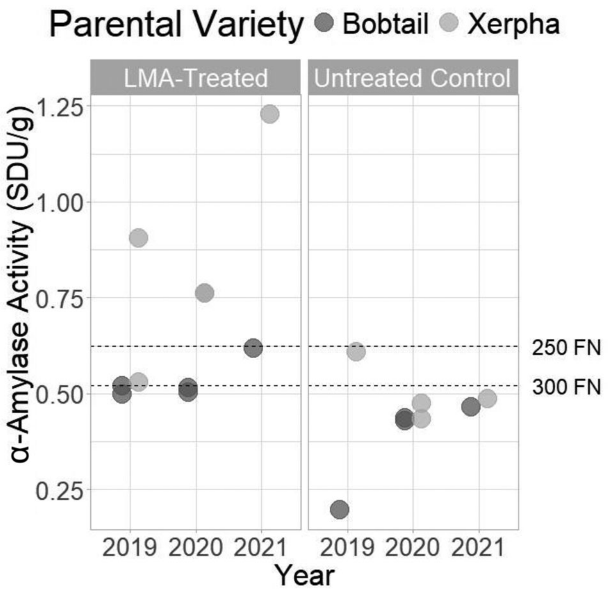

FIGURE 2 Late-maturity α-amylase (LMA) induction of parent lines across years; Bobtail (dark gray) and Xerpha (light gray) sample distribution of cube root transformed α-amylase activity (SDU/g) for all three field seasons. Five LMA-induction replicates ($n = 10$) and four untreated field replicates ($n = 8$) were performed in 2019, 2020, or 2021. FN, falling number; SDU, sprout damage units.

The reproducibility of field experiments was assessed by calculating Pearson's correlation coefficients for the cube root transformed α-amylase activity within and between years for both LMA-treated and -untreated replicates (Table 3; Tables S7 and S8). LMA-treated replicates exhibited moderate to high correlations within single years, and low, though significant, correlations between years (Table S7). The LMA-treated replicates from the 2020 field season showed a slightly higher and more significant correlation between replicates than LMA-treated replicates from 2019 ($R = 0.662$, $p = 4.36 \times 10^{-23}$ and $R = 0.539$, $p = 4.93 \times 10^{-11}$, respectively). The 2019 LMA-treated replicates had low but significant correlations to 2020 LMA-treated ($R = 0.164$–0.253, $p < 0.05$) and 2021 LMA-treated replicates ($R = 0.193$–0.258, $p < 0.05$). The highest correlation between years was $R = 0.348$, $p = 3.1 \times 10^{-6}$ between 2020.LMA2 and 2021.LMA1. The average α-amylase activity for LMA-treated replicates demonstrated a moderate to high and highly significant correlation between all LMA-treated replicates (Figure 3; Table S7). While untreated samples showed less variation for α-amylase activity than treated samples, it was still possible to observe correlations within and between years (Figure ; Table S8). For example, the two 2020 untreated replicates were significantly correlated ($R = 0.801$, $p = 6.59 \times 10^{-40}$). Untreated samples in 2019, 2020, and 2021 showed significant-moderate cross-year correlations (Table S8). Untreated replicates were more highly correlated across years than the LMA-treated replicates (Table 3; Tables S7 and S8).

Interestingly, only two correlations were observed between treated and untreated samples, suggesting low overlap in the sources of variation between both treatment groups. The average α-amylase activity of LMA-treated replicates across all years had low and nonsignificant correlations with the untreated controls across all years (Table 3; Figures S4 and S5). LMA-treated and -untreated replicates within years were not significantly correlated. Replicate 2021.LMA1, which had the highest average α-amylase activity across years, had a low but significant correlation with the untreated average across all years and the 2020 untreated average (Table 3). Examination of reproducibility between replicates, years, and treatments using Pearson's correlations suggested that while there was a high degree of year-to-year variation, the experiments were measuring a reproducible trait.

TABLE 4 Ten quantitative trait loci (QTLs) identified via compositive interval mapping and four markers identified via single marker association mapping associated with α-amylase activity from LMA-treated and -untreated samples.

	CIM Identified QTL[a]								
QTL name	**Traits**	**Chr**	**LOD**	**Effect**	**Peak (cM)**	**Interval (cM)**	**R^2**	**Left marker**[b]	**Right marker**[b]
QLcon-wsu.2A[c]	U LMA Freq.	2A	3	0.044	7.51	3.4	0.0676	2A_14299680	2A_34105730
	Average U all years	2A	3.5	0.014	7.51	3.8	0.073	2A_14299680	2A_34105730
	U BLUP	2A	3.5	0.009	7.51	3.7	0.0761	2A_14299680	2A_34105730
QLcon-wsu.3A[c]	Average U 2019	3A	3	0.05	79.41	5.6	0.0673	3A_431422512	3A_509564326
QLind-wsu.3B.1[d]	Average LMA Ind. 2020	3B	4.1	−0.06	15.61	5.9	0.0818	3B_59889587	3B_59485849
QLcon-wsu.3B.2[c]	2020.U1	3B	3.6	0.016	49.81	3.2	0.0746	3B_761588835	3B_762022660
	Average U 2020	3B	3.6	0.016	50.01	2.3	0.0725	3B_761588835	3B_761833638
QLind-wsu.5B[d]	Average LMA Ind. all years	5B	3.5	−0.05	11.81	6.4	0.0756	5B_24648800	5B_16725511
	Average U all years	5B	3.6	−0.01	20.31	2.7	0.0728	5B_26845670	5B_28755249
	2020.U2	5B	3.6	−0.02	20.31	2.5	0.0746	5B_26845670	5B_28755249
QLind-wsu.6B[d]	Average LMA Ind. 2020	6B	4.4	0.082	13.61	6.7	0.0873	6B_48151735	6B_48106865
QLind-wsu.7A.1[d]	LMA Ind. LMA Freq.	7A	3.8	−0.08	28.11	2.7	0.0804	7A_27614565	7A_30089367
QLind-wsu.7A.2[d]	2020.LMA1	7A	5.6	−0.07	62.81	0.7	0.1211	7A_76800924	7A_77491640
	Average LMA Ind. 2020	7A	6.7	−0.08	62.81	0.7	0.1504	7A_76800924	7A_77491640
	2020.LMA1	7A	4.6	−0.06	70.61	1.6	0.0993	7A_116698496	7A_133643468
QLind-wsu.7A.3[d]	LMA Ind. LMA Freq.	7A	4.2	0.081	97.01	3.1	0.084	7A_622828170	7A_634878887
	LMA Ind. LMA Freq.	7A	4.1	0.082	103.01	0.8	0.088	7A_640164758	7A_642424915
QLind-wsu.7D[d]	Average LMA Ind. 2019	7D	3.3	−0.05	77.11	15.6	0.0745	7D_612424325	7D_629692367
	SM Identified QTL[e]								
Significant marker	**Trait**	**Chr**	**LOD**	**Effect**	**Peak (cM)**	**Interval (cM)**	***p*-value**	**Left marker**[b]	**Right marker**[b]
7A_24618513[d]	LMA Ind. LMA Freq.	7A	3.2	−0.38	21.61	3	***	7A_24618513	7A_23810520
7A_85902743[d]	2020.LMA1	7A	3.4	−0.06	62.81	0.9	***	7A_85902743	7A_77491640
7A_85902743[d]	Average LMA Ind. 2020	7A	3.5	−0.06	62.81	1	**	7A_85902743	7A_77491640
7A_116530568[d]	2020.LMA1	7A	3	−0.05	68.61	2.7	***	7A_116530568	7A_115326808
Rht-B1[c]	Average U all years	4B	3.3	0.015	0.01	18.3	**		
Rht-B1[c]	2020.U1	4B	3.3	0.018	0.01	17.9	**		
Rht-B1	Height (cm)	4B	7.4	8.949	0.01	16.1	***		

Note: Years with single replicates are designated as U1 and U2 for untreated replicates or LMA1 and LMA2 for LMA-induced replicates.

Abbreviations: Chr, chromosome; Freq., frequency; Ind., induced; LOD, logarithm of odds.

[a] QTL identified using composite interval mapping (CIM).

[b] Physical position (bp) indicated in marker name after underscore.

[c] QTL associated with constitutive expression of α-amylase.

[d] QTL associated with cold shock-induced expression of α-amylase.

[e] QTL identified using single marker (SM) analysis.

** and *** depict significance at the 0.01 and 0.001 probabilities levels.

3.2 | Sources of variation in LMA phenotype

An REML method was employed to model the factors contributing to variation within treatment groups between annual field trials and to calculate BLUPs given the limited correlation between replicates from different years (Table S4). The treatment type and year were significant contributors to phenotypic variation, explaining 25.4% and 7.3% of the total phenotypic variation, respectively (Table 2). Genotype accounted for ∼15% of the total phenotypic variation and was a significant factor in variation of α-amylase activity; residual error was less than 8% (Table 2). Interactions between genotype and year, genotype and treatment type, and genotype, year, and treatment type were also identified as significant factors (14%, 11.5%, and 11.7%) (Table 2). A small yet significant interaction between year and treatment type was

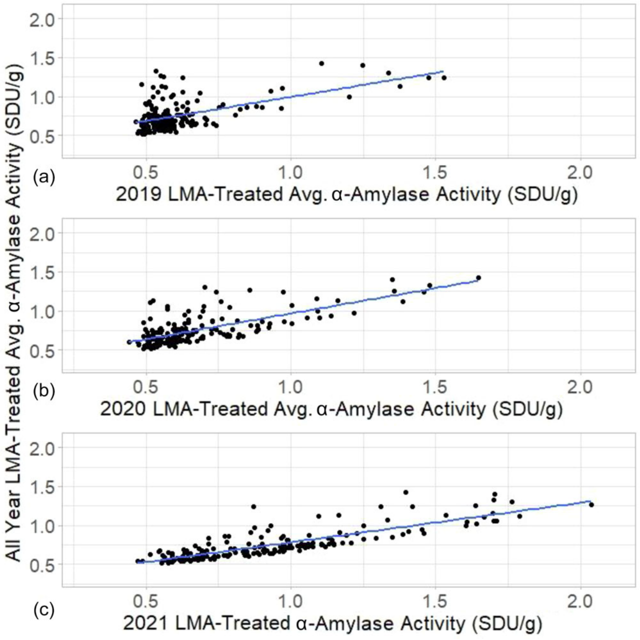

FIGURE 3 Linear regression and scatter plots comparing the cube root transformed average α-amylase activity (SDU/g) of late-maturity α-amylase (LMA)-treated replicates across all years to three independent LMA-treated experiments: (a) average α-amylase for LMA-treated replicates in 2019 ($p = 6.5 \times 10^{-16}$), (b) average α-amylase activity for LMA-treated replicates in 2020 ($p = 1.9 \times 10^{-28}$), and (c) α-amylase activity for 2021 LMA-treated replicate ($p = 1.2 \times 10^{-45}$). Avg., average; SDU, sprout damage units.

observed that explained 6.6% of the total variation in the model.

The impact of reduced height (*Rht*) alleles *Rht-B1* and *Rht-D1*, awn-type, and anthesis date were examined independently of genotype using one-way ANOVAs (Table S3). The biparental population segregated for both *Rht-B1b* or the *Rht-D1b* semidwarfing alleles, enabling us to examine the effects of the tall *Rht-B1a*/*Rht-D1a* *wt*, each semidwarfing allele *Rht-B1b* or *Rht-D1b*, and the double dwarf *Rht-B1b*/*Rht-D1b* genotypes on LMA phenotype. When both LMA-treated and -untreated samples were considered, the *Rht-B1* genotype alone did not have a significant effect on α-amylase activity, whereas the *Rht-D1* genotype was slightly significant ($p = 0.0002$). Both *Rht-B1* and *Rht-D1* genotypes showed significant interactions with treatment type ($p = 0.0026$ and $p = 8.77 \times 10^{-7}$, respectively), though not with year. When the combined *Rht-B1 Rht-D1* genotype ("*Rht* Read") was considered, this single factor had a more significant effect on α-amylase activity than either gene individually ($p = 2.46 \times 10^{-12}$) and showed significant interaction with treatment type but had no significant interaction with year ($p = 8.0 \times 10^{-5}$ and $p = 0.58$) (Table S3). *Rht* Read captured the effect of the combined genes as substituting the term with an interaction between *Rht-B1* and *Rht-D1* did not alter ANOVA results.

When untreated, *wt* tall (*Rht-B1a/Rht-D1a*) lines had slightly higher average α-amylase activity than either one-gene or two-gene (*Rht-B1b/Rht-D1b*) dwarf lines, though variation in α-amylase activity between lines with different *Rht* genes had no or low significance (Figure 5). In LMA-treated samples, *Rht-B1b/Rht-D1b* double-mutant dwarf lines consistently had a higher average α-amylase activity than *wt* tall (*Rht-B1a/Rht-D1a*) or single homozygous mutant (*Rht-B1b/Rht-D1a* or *Rht-B1a/Rht-D1b*) semidwarf lines (Figure 5; Table S3). This result was most significant in 2021 where tall and single-gene dwarf lines had comparable levels of α-amylase activity with an average α-amylase activity equivalent to 112–127 s FN, whereas double-mutant dwarf lines had an average α-amylase activity equivalent to an FN of 80 s (Figure 5). This suggests that regulation of LMA by DELLA proteins is more complex than an off-versus-on regulatory switch. Plant height as measured in 2020 did not have a significant association with α-amylase activity ($p = 0.143$) but had significant interactions with treatment type ($p = 9.83 \times 10^{-5}$) (Table S3). The presence or absence of awns did not significantly contribute to variation in α-amylase activity ($p = 0.52$), though there was a slightly significant interaction between awn presence and treatment type ($p = 0.04$). Anthesis date exhibited a weak yet significant association with α-amylase activity ($p = 0.005$), possibly due to variation in ambient temperatures when different varieties reached the LMA-susceptible developmental stage (Table S3). The inclusion of plant height, presence of awns, anthesis date, or combined *Rht* genotype did not significantly improve model fit and were excluded from the final MLM used to calculate BLUPs and heritability.

Variation in LMA phenotypes can be explained by both genotype and environment. Due to the limited replication in certain years, BLUPs were calculated across all years separately for LMA-treated and -untreated samples using genotype and year as factors in the MLM. Repeatability, estimated as broad-sense heritability (H^2), was also calculated separately for both treatment types. A repeatability of 0.81 and 0.66 for untreated and LMA-treated replicates, respectively, suggested that a QTL-mapping study was feasible. Much of the unexplained residual variation in LMA induction may be due to differences in environmental conditions between years or to unaccounted for variation within the field. We examined air temperature, RH, and precipitation data from WSU AgWeatherNet's Pullman, WA, station for a period of 8 weeks in 2019, 2020, and 2021 as the headrows reached soft-dough stage (Table S2; Rasul et al., 2015). The maximum temperature during this time in 2019 and 2020 was 85°F/29.4°C, while 2021 had a maximum temperature of 105°F/40.5°C. The 2021 field season was characterized by heat and drought stress leading up to collection of LMA-

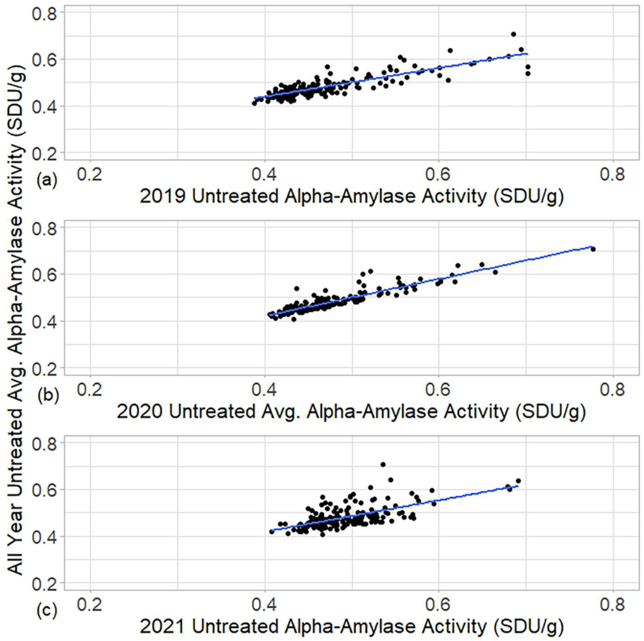

FIGURE 4 Linear regression and scatter plots comparing the cube root transformed average α-amylase activity (SDU/g) of untreated replicates across all years to three independent field seasons: (a) α-amylase for untreated samples in 2019 ($p = 1.2 \times 10^{-48}$), (b) average α-amylase activity for untreated replicates in 2020 ($p = 9.4 \times 10^{-68}$), and (c) α-amylase activity for 2021 untreated samples ($p = 3.6 \times 10^{-20}$). Avg., average; SDU, sprout damage units.

treated material before a rainfall event of 0.2 in. as lines were reaching the soft-dough stage. The higher field temperatures mean that the starting temperatures were higher in 2021 so that the LMA treatment involved a greater decrease in temperature. In 2019 and 2020, a few small rainfall events happened during the same window, but cumulative precipitation did not exceed 0.15 in. Despite the rainfall in 2021, sprouting does not appear to be a contributing factor to the high levels of LMA expression due to the low levels of α-amylase activity in the untreated material left to mature in the field (Figure 1; Table 1).

3.3 | QTL analysis

Linkage maps were constructed using the 3022 polymorphic SNP markers from GBS and the 40 SSR markers on chromosomes 3A, 3B, 5A, 6B, 7A, and 7B (Table S6). The SSR markers were selected to increase marker density in LMA-associated regions based on previous mapping studies and a preliminary SM QTL analysis (reviewed by Cannon et al., 2022; Figure S6; Table S6). Mapping identified 21 linkage groups with 1553 markers, for a total map length of 2440 cM and an average marker density of 0.64 markers/cM with one linkage group per chromosome (Table S6). A QTL analysis was conducted to identify markers associated with LMA resistance and susceptibility in the Xerpha/Bobtail bi-parental mapping population using CIM and SM analysis in QTL Cartographer. A total of 18 sets of phenotypic data were analyzed, including BLUPs for untreated and treated replicates across all years, LMA incidence across all replicates in LMA-treated and -untreated lines, cube root transformed α-amylase activity for each replicate, average α-amylase activity for replicates of the same year and treatment type, and average α-amylase activity across years within treatments (Table S1).

A robust association between multiple traits and the *Rht-B1* locus on chromosome 4B was revealed by SM analysis (Table 4). Plant height exhibited the strongest association (LOD = 7.37), although the average untreated α-amylase activity values across all years and in 2020.U1 were also significantly associated with *Rht-B1* (Table 4). Four other traits were mapped by SM analysis to loci on 7A that co-located with two of the three QTL mapped using CIM. Ten total QTLs were detected using CIM with LOD thresholds determined via 600 permutations. Among these, two QTLs were associated with α-amylase activity in untreated (U) replicates, while the remaining eight QTLs were associated with α-amylase activity in LMA-treated replicates (LMA) (Table 4). One major significant QTL was detected and mapped to chromosome 7A using the 2020 LMA-treated average α-amylase activity and one 2020 LMA-treated replicate (2020.LMA1). The remaining nine QTLs had minor associations with α-amylase activity and were distributed across chromosomes 2A, 3A, 3B, 5B, 6B, 7A, and 7D. Incidence of LMA in LMA-treated material mapped two minor QTLs to unique loci on 7A. The BLUPs of untreated replicates mapped a QTL to chromosome 2A, whereas the LMA-treated BLUPs did not map any QTL. The remaining QTLs were identified using the cube root transformed values for average (within and across years) or individual LMA-treated and -untreated replicates. Notably, no datasets from 2021 mapped significant QTL; the majority of detected QTLs were mapped by the average or individual LMA-treated replicates from 2020. The only QTLs mapped using data from 2019 were *QLcon-wsu.3A* (*QTL LMA constitutive-wsu.3A* from untreated data) and *QLind-wsu.7D* (*QTL LMA-induced-wsu.7D*) from cold-treated data.

4 | DISCUSSION

To identify QTL for LMA tolerance that can be used to develop markers for MAS, we conducted the first mapping study of LMA tolerance in a winter wheat biparental RIL population. A previous genome-wide association study identified LMA QTL in a panel of 251 North American hard spring varieties that included germplasm from the US PNW, but this is the first biparental winter wheat population used to map tolerance from this region (Liu, Parveen et al., 2021).

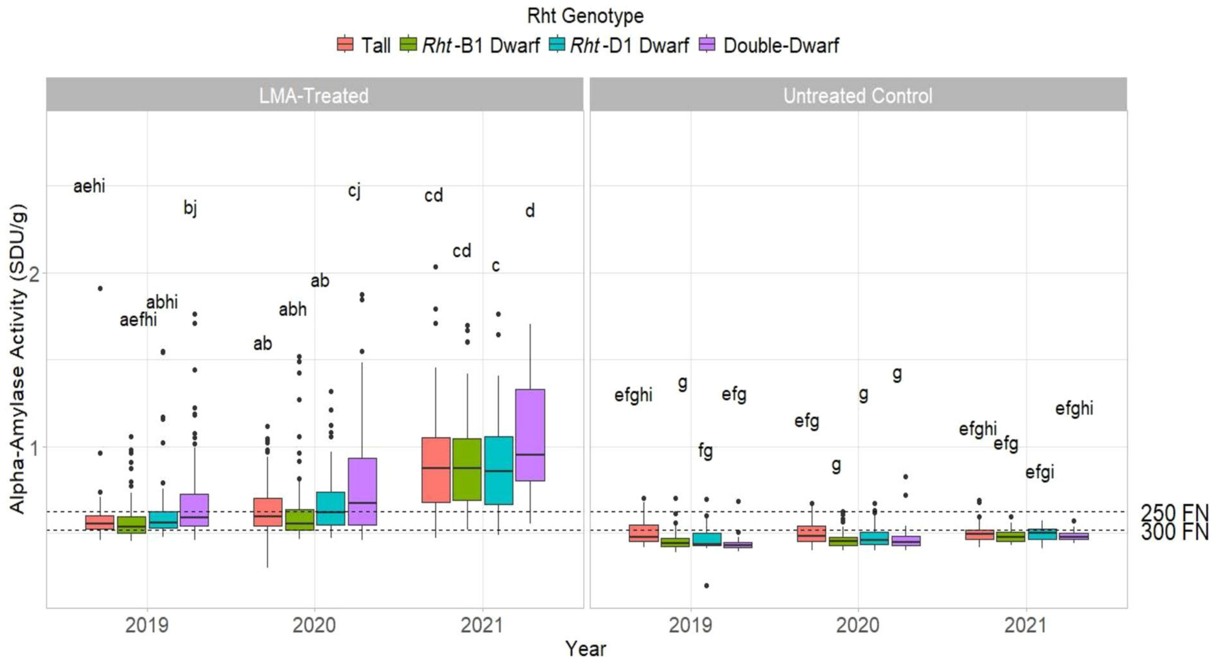

FIGURE 5 Late-maturity *α*-amylase (LMA)-treated and -untreated/control replicate *α*-amylase activity (SDU/g) by combined *Rht-B1* and *Rht-D1* genotype. *α*-Amylase expression is plotted for both LMA-treated and -untreated replicates for all 3 years. Tall (*Rht-B1a/D1a*), semidwarfs (*Rht-B1b/D1a* and *Rht-B1a/D1b*), and double dwarfs (*Rht-B1b/D1b*) are plotted from left to right each year in red, green, blue, and purple. Similarity of groups is indicated by letters above individually plotted boxplots as calculated by Tukey honestly significance difference test. FN, falling number; *Rht*, reduced height; SDU, sprout damage units.

Variation in field environment appeared to significantly influence whether LMA was induced in a given line. Variation in precipitation and temperature between years appeared to contribute more to year-to-year variation in LMA-treated than -untreated material (Figures 3 and 4). Heat stress was an important factor in 2021 when the maximum temperature reached 105°F/40.5°C the week before LMA induction, resulting in a temperature difference of 22.5°C between field and growth chamber conditions (Table S2; Rasul et al., 2015). This is nearly twice the temperature differential experienced in 2019 and 2020 when maximum temperatures did not exceed 85°F/29.4°C. Future work will need to determine if the larger temperature change, such as that which occurred in 2021, is always associated with a higher proportion of lines inducing LMA and a higher average *α*-amylase activity. Consistent with this observation, Liu, Tuttle et al. (2021) found that a larger difference between basal and induction temperatures gave a higher fold-increase in *α*-amylase. The correlation between treated and untreated replicates increased as the proportion of lines exhibiting an LMA phenotype increased, as seen in 2021 (Figures S4 and S5; Table 3). It is possible that in some backgrounds LMA tolerance is not so much absolute resistance as a requirement for a bigger temperature differential to induce LMA. For example, under cool-treated conditions, the LMA-tolerant parent Bobtail induced LMA in 2021 but not in 2019 and 2020 (Figure 2). In contrast, the LMA-susceptible Xerpha parent consistently induced LMA. Although there were measurable differences in *α*-amylase activity between the parents in 2021, no QTLs were mapped with LMA-treated data. LMA induction in most lines in 2021 may have led to failure to map LMA tolerance. Alternatively, a higher proportion of the variation in *α*-amylase expression may have been due to heat-associated field variation in 2021. In fact, one portion of the field could not be collected in 2021 because it was too dry.

Despite the significant year-to-year environmental variation, there was a high degree of reproducibility within replicates and between years achieved through implementation of improved LMA phenotyping and statistical methods (Butler et al., 2009; A. P. Derkx & Mares, 2020; Liu, Tuttle et al., 2021). The untreated and LMA-treated *α*-amylase levels showed a heritability of 81% and 66%, respectively. This was associated with moderate levels of correlation between independent field trials (Table 3; Tables 7 and 8). Mapping *α*-amylase expression in both untreated and LMA-inducing environments enabled identification of QTL capable of controlling LMA across diverse environments. A total of 10 QTLs were identified (LOD > 3.0).

Three markers identified as significant co-localized with *QLind-wsu.7A.1* (marker 7A_24618513) and *QLind-wsu.7A.2* (markers 7A_85902743 and 7A_116530568) identified by CIM (Figure 6; Table 4). Of the 10 QTLs identified in the current study, only *QLcon-wsu.3A*, *QLcon-wsu.3B.2*, and *QLind-wsu.6B* appear to co-locate

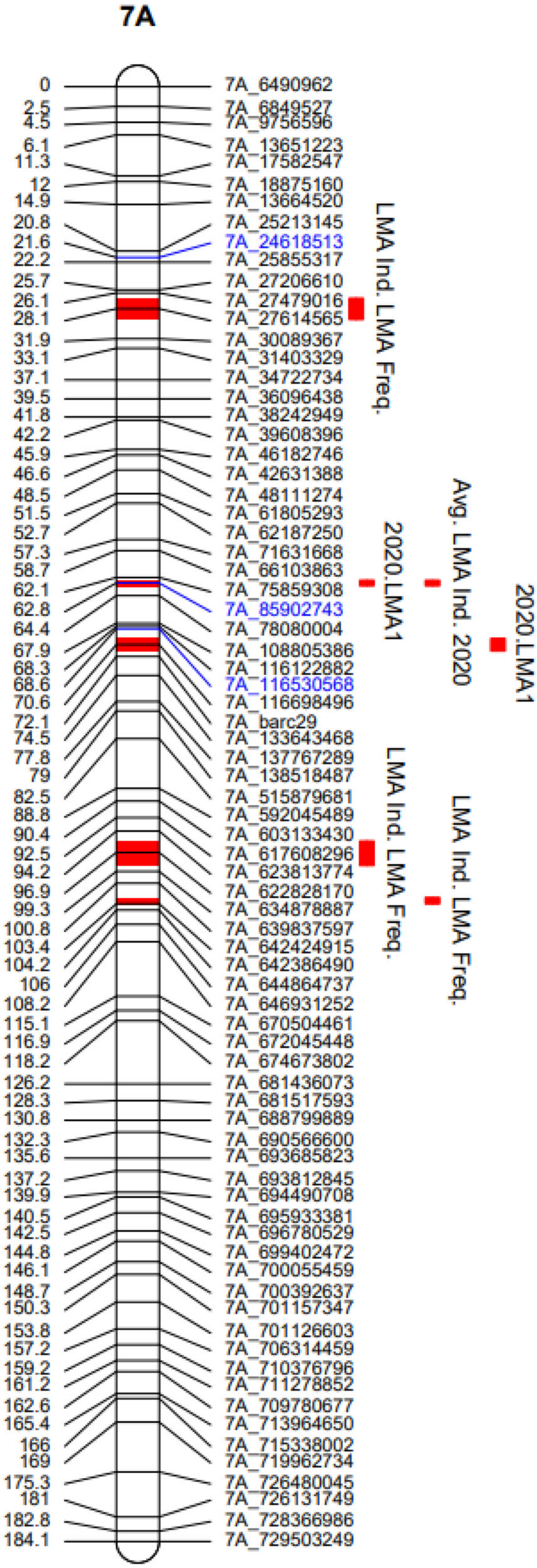

FIGURE 6 Genetic maps showing three quantitative trait loci (QTLs) for α-amylase in late-maturity α-amylase (LMA)-treated material. Significant markers from single marker (SM) analysis are shown in blue, while QTL intervals detected via composite interval mapping (CIM) are indicated in red on the chromosome. Position in cM

(Continues)

FIGURE 6 (Continued) is indicated on the left, with the mapped trait, as well as 1 and 2 logarithm of odds (LOD) confidence intervals for each QTL on the right. Only marker names every 2 cM intervals are displayed; full linkage maps are available in Table S2. Avg., average; Freq., frequency; Ind., induced.

with existing LMA-associated QTL based on the physical position of markers in the Chinese Spring v1.0 genome and SSR maps (Emebiri et al., 2010; Fairlie et al., 2024; IWGSC, 2018; Liu, Parveen et al., 2021; D. Mares et al., 2023; McNeil et al., 2009; Mohler et al., 2014; Mrva & Mares, 2001b; Tan et al., 2010; Verblya & Cullis, 2012; Wang et al., 2014; J. Zhang et al., 2014). The remaining 7 QTLs represent novel LMA-associated QTLs, which may be characteristic of LMA tolerance in winter wheat or of US PNW germplasm (Table 4).

Three QTLs were mapped to chromosome 7A: two minor QTLs (*QLind-wsu.7A.1* and *QLind-wsu.7A.3*) and one major QTL (*QLind-wsu-7A.2*) (Figure 6). The two minor QTLs were mapped to the short and long arms of 7A by LMA incidence in LMA-induction material and appeared distinct from previously reported QTLs. As LMA incidence serves as an index for consistency of LMA expression across years, these QTLs may provide broad control of α-amylase across environments. *QLind-wsu.7A.2*, the most significant QTL identified (max LOD 6.7), was mapped with LMA induction data from 2020 to the long arm of 7A (Figure 6; Table 4). The previously published major QTL *LMA-1* on chromosome 7B was not identified in this population (A. Derkx et al., 2021). Thus, the strong effect of *QLind-wsu.7A.2* may provide a good alternative marker for winter wheat breeding. Future work will need to characterize this QTL in a wider range of winter wheat varieties. While future work will need to fine map this QTL, the 0.69 Mb *QLind-wsu.7A.2* interval contained 10 annotated genes including an ethylene-responsive element binding factor (AP2/ERF domain protein) and a chloroplastic/amyoplastic starch synthase gene (Qi et al., 2011; Yates et al., 2022).

Interesting QTLs were detected on group 3 and 5 chromosomes (Figure 7; Table 4). Possibly, the most reproducible QTL was *QLind-wsu.5B* (LOD 3.5) because it was detected using both LMA-treated and -untreated data averaged across all years, suggesting that it decreases α-amylase levels under a wide range of environments (Figure 7; Table 4). *QLcon-wsu.3A* was detected near the centromere of chromosome 3A and appeared to overlap with previously detected LMA, PHS, and dormancy loci (Kulwal et al., 2004; Kumar et al., 2015; Mohan et al., 2009; Tan et al., 2010; Zuo et al., 2019). *QLind-wsu.3B.1* mapped to the short arm, while *QLcon-wsu.3B.2* mapped to the long arm of chromosome 3B. Both QTLs on 3B span intervals of approximately 0.4 Mb containing

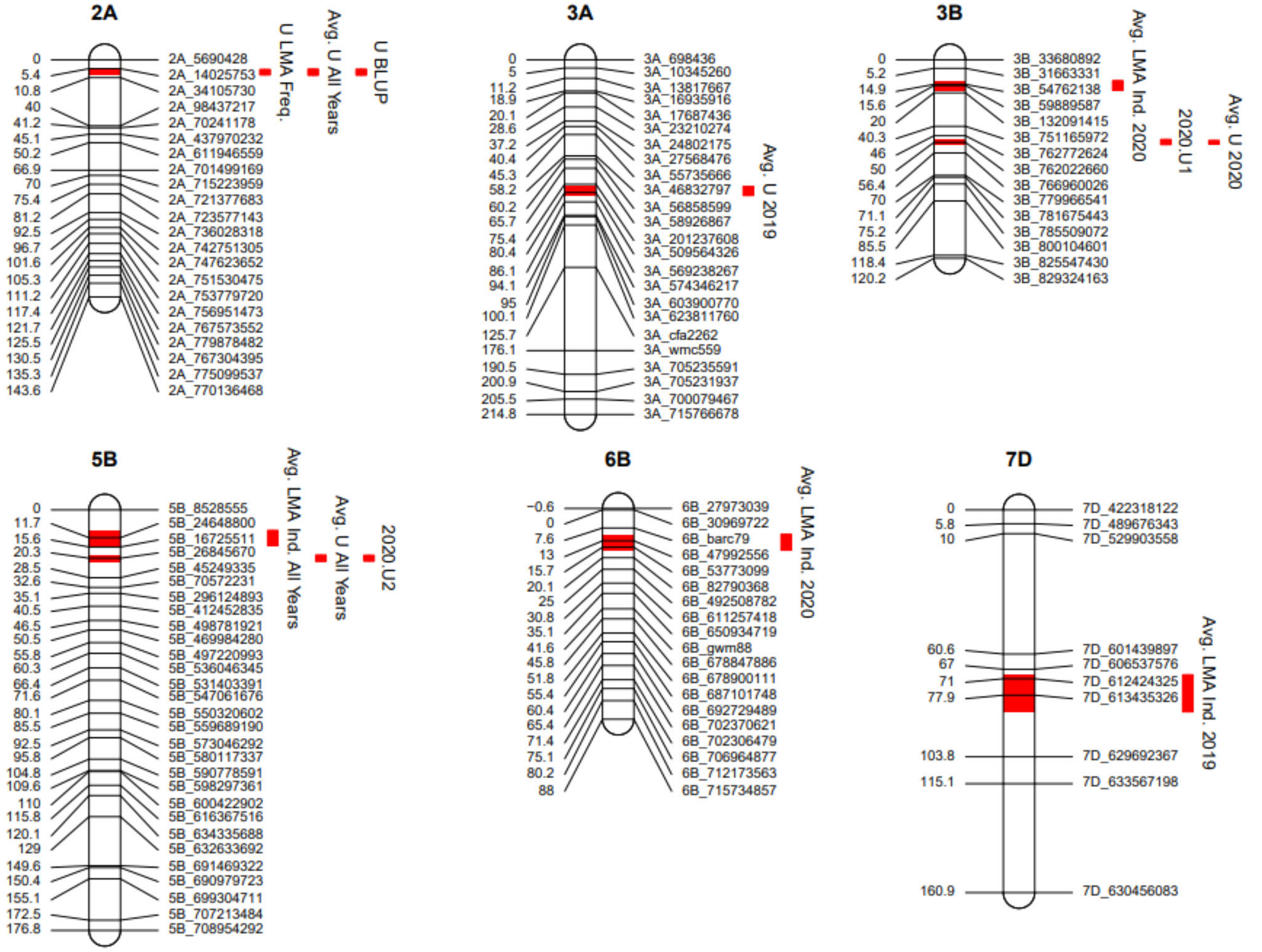

FIGURE 7 Genetic maps showing seven quantitative trait loci (QTLs) for α-amylase activity. Position in cM is indicated on the left, and the QTL interval is indicated by colored interval on the chromosome, with the mapped trait, as well as 1 and 2 logarithm of odds (LOD) confidence intervals for each QTL on the right. Only marker names every 5 cM intervals are displayed; full linkage maps are available in Table S2. Avg., average; Freq., frequency; Ind., induced; LMA, Late-maturity α-amylase.

annotated genes involved in plant development and abiotic stress responses, including a BTB/POZ domain and BURP domain proteins (Shalmani et al., 2021; Yates et al., 2022; Zhu, 2022). Due to its proximity to the centromere, large size, inconsistent association with markers, and tendency to map to opposite arms of 3B, it is possible the previously reported major LMA-associated QTL on 3B is more than one significant locus (Liu, Parveen et al., 2021; McNeil et al., 2009; Mrva & Mares, 2001a; Tan et al., 2010; Verblya & Cullis, 2012; J. Zhang et al., 2014). *QLcon-wsu.3B.2* may co-locate with this major LMA QTL on 3B that may be homoeologous with *QLcon-wsu.3A*. *QLind-wsu.3B.1* appears to be a novel QTL on the short arm of 3B further from the centromere than any previously reported QTLs.

The remaining three minor QTLs were *QLcon-wsu.2A*, *QLind-wsu.6B*, and *QLind-wsu.7D*. *QLcon-wsu.2A* was mapped using untreated material to the short arm of chromosome 2A (Figure 7). Previous studies mapped LMA-associated QTL to the long arms of chromosomes 2A and 5B, suggesting *QLcon-wsu.2A* and *QLind-wsu.5B* are unique (Mohler et al., 2014; Tan et al., 2010; Verblya & Cullis, 2012). The *QLind-wsu.6B* locus mapped to the short arm of 6B and did not co-locate with the *α-amy-B1* candidate gene proposed for the 6B LMA QTL published in previous studies (Bevan, 2020; Emebiri et al., 2010; Liu, Parveen et al., 2021; Mohler et al., 2014). *QLind-wsu.7D* mapped to the opposite arm than was reported in North American spring wheat but this study, as well as recent reports in Australian germplasm, validate that the 7D chromosome plays a role in LMA expression (Fairlie et al., 2024; Liu, Parveen et al., 2021; D. Mares et al., 2023; Figure 7).

The observed suppressive effect of *Rht-B1b* and *Rht-D1b* alleles on α-amylase expression under untreated conditions is consistent with previously published findings (Figure 5).

The unexpected observation that *Rht-B1b/Rht-D1b* double-dwarf lines exhibited higher α-amylase levels than *wt* (tall) and single-gene semidwarf lines in response to cold is contrary to prior notions and suggests that DELLA mutations may enhance cold sensitivity rather than merely suppress LMA at higher temperatures in winter wheat. This cold-activated mechanism for bypassing the gain-of-function DELLA mutation repression of α-amylase expression may be either GA-dependent or GA-independent (D. Mares et al., 2022). This aligns with findings by Pereira et al. (2002), where a 2°C cold treatment "rescued" coleoptile elongation across *wt*, semidwarf, and double-dwarf *Rht* mutants; *Rht* isolines also showed increased sensitivity to GA across a wider range of GA concentrations than at warm 18°C. The dormancy-breaking treatment of cold stratification appears to stimulate germination in part through increased GA sensitivity and levels (Martinez et al., 2016; Tuttle et al., 2015; Xu et al., 2016; Yamauchi et al., 2004). Since α-amylase expression occurs during germination, this cold temperature "rescue" of GA-sensitivity or GA signaling may be mechanistically related to LMA induction. Future work could examine this using near-isogenic lines and/or using targeted mutations in *Rht-B1*, and *Rht-D1*. Further research into these mechanisms will be required to fully characterize the temperature-dependent regulation of LMA-expression.

This study identified multiple QTLs with potential roles in the cold-dependent and -independent mechanisms for regulating total α-amylase expression under both normal field and LMA-inducing conditions. Light was also shed on the temperature-dependent nature of GA sensitivity regarding LMA expression. Future studies should prioritize mapping LMA tolerance under both warm and LMA-inducing cold conditions to individually characterize both LMA mechanisms and their relative contributions to total α-amylase levels. Moreover, near-isogenic lines would be beneficial for precisely defining the differential effects of single and double (*Rht-B1b*/*Rht-D1b*) mutants on LMA induction. Employing a biparental mapping population where both parents are double dwarfs (*Rht-B1b*/*Rht-D1b*) would allow identification of LMA regulators downstream of DELLA. The precision of the QTL detected in the Xerpha × Bobtail population contrasts with many previously detected QTLs, which had much broader intervals. This precision will be useful in fine mapping causative genes. Future work will develop these QTLs for MAS and assess their effectiveness in selection for LMA tolerance in PNW germplasm.

AUTHOR CONTRIBUTIONS

Elliott J. Marston: Data curation; formal analysis; investigation; methodology; software; visualization; writing—original draft; writing—review and editing. **Marcus A. Hooker**: Data curation; formal analysis; methodology; software; writing—review and editing. **Karol Marlowe**: Investigation; writing—review and editing. **Travis R. Ruff**: Investigation; writing—review and editing. **Yan Liu**: Investigation; writing—review and editing. **Scott W. Carle**: Formal analysis; investigation; visualization; writing—review and editing. **Rehana S. Parveen**: Data curation; investigation; methodology. **Susanne Trittinger**: Resources; writing—review and editing. **Deven R. See**: Conceptualization; supervision; writing—review and editing. **Camille M. Steber**: Conceptualization; data curation; investigation; methodology; supervision; writing—review and editing.

ACKNOWLEDGMENTS

The authors would like to thank Robert Zemetra and Andrew Ross in the College of Agricultural Sciences at Oregon State University for providing access to the Xerpha × Bobtail mapping population. We thank Patricia DeMacon and Kimberly Garland-Campbell for planting and maintaining field headrows. We thank members of the Steber and Garland-Campbell lab for assistance with field sampling. We thank members of the Steber and See lab for helpful comments on the manuscript. This work was funded by the USDA-ARS.

CONFLICT OF INTEREST STATEMENT

The authors declare no conflicts of interest.

ORCID

Elliott J. Marston https://orcid.org/0000-0002-8238-2107
Karol Marlowe https://orcid.org/0000-0001-5948-196X
Scott W. Carle https://orcid.org/0000-0001-9885-5565
Susanne Trittinger https://orcid.org/0000-0002-5952-8200
Deven R. See https://orcid.org/0000-0002-1577-2949
Camille M. Steber https://orcid.org/0000-0001-6255-7670

REFERENCES

Allan, R. E. (1986). Agronomic comparisons among wheat lines nearly isogenic for three reduced-height genes. *Crop Science*, *26*, 707–710. https://doi.org/10.2135/cropsci1986.0011183x002600040014x

Barrero, J. M., Mrva, K., Talbot, M. J., White, R. G., Taylor, J., Gubler, F., & Mares, D. J. (2013). Genetic, hormonal, and physiological analysis of late maturity α-amylase in wheat. *Plant Physiology*, *161*(3), 1265–1277. https://doi.org/10.1104/pp.112.209502

Barrero, J. M., Porfirio, L., Hughes, T., Chen, J., Dillon, S., Gubler, F., & Ral, J. P. F. (2020). Evaluation of the impact of heat on wheat dormancy, late maturity alpha-amylase and grain size under controlled conditions in diverse germplasm. *Scientific Reports*, *10*(1), Article 17800. https://doi.org/10.1038/s41598-020-73707-8

Bates, D., Mächler, M., Bolker, B., & Walker, S. (2014). Fitting linear mixed-effects models using lme4. *arXiv*. https://doi.org/10.48550/arXiv.1406.5823

Bevan, J. G. (2020). *Comparative QTL mapping of Hagberg falling number, pre-harvest sprouting, and late maturity α-amylase in UI platinum by SY capstone derived population* [Master's thesis, University of Idaho]. University of Idaho Library. https://www.lib.uidaho.edu/digital/etd/items/bevan_idaho_0089n_11827.html

Börner, A., Nagel, M., Agacka-Mołdoch, M., Gierke, P. U., Oberforster, M., Albrecht, T., & Mohler, V. (2018). QTL analysis of falling number and seed longevity in wheat (*Triticum aestivum* L.). *Journal of Applied Genetics*, *59*(1), 35–42. https://doi.org/10.1007/s13353-017-0422-5

Bradbury, P. J., Zhang, Z., Kroon, D. E., Casstevens, T. M., Ramdoss, Y., & Buckler, E. S. (2007). TASSEL: Software for association mapping of complex traits in diverse samples. *Bioinformatics*, *23*(19), 2633–2635. https://doi.org/10.1093/bioinformatics/btm308

Brownstein, M. J., Carpten, J. D., & Smith, J. R. (2018). Modulation of non-templated nucleotide addition by *Taq* DNA-polymerase: Primer modifications that facilitate genotyping. *Biotechniques*, *20*(6), 1004–1010. https://doi.org/10.2144/96206st01

Butler, D. G., Tan, M. K., & Cullis, B. R. (2009). Improving the accuracy of selection for late maturity α-amylase in wheat using multi-phase designs. *Crop Pasture Science*, *60*(12), 1202–1208. https://doi.org/10.1071/CP09124

Cannon, A. E., Marston, E. J., Kiszonas, A. M., Hauvermale, A. L., & See, D. R. (2022). Late-maturity α-amylase (LMA): Exploring the underlying mechanisms and end-use quality effects in wheat. *Planta*, *255*(1), Article 2. https://doi.org/10.1007/s00425-021-03749-3

Carle, S. W. (2020). *Freezing tolerance and genetic marker maps in wheat* [Doctoral dissertation, Washington State University]. Washington State University Dissertations & Theses. https://rex.libraries.wsu.edu/esploro/outputs/99900581701801842

Cheng, C. R., Oldach, K., Mrva, K., & Mares, D. (2014). Analysis of high pI *α-Amy-1* gene family members expressed in late maturity α-amylase in wheat (*Triticum aestivum* L.). *Molecular Breeding*, *33*(3), 519–529. https://doi.org/10.1007/s11032-013-9968-z

Derkx, A., Baumann, U., Cheong, J., Mrva, K., Sharma, N., Pallotta, M., & Mares, D. (2021). A major locus on wheat chromosome 7B associated with late-maturity α-amylase encodes a putative *ent*-copalyl diphosphate synthase. *Frontiers in Plant Science*, *12*, Article 637685. https://doi.org/10.3389/fpls.2021.637685

Derkx, A. P., & Mares, D. J. (2020). Late-maturity α-amylase expression in wheat is influenced by genotype, temperature and stage of grain development. *Planta*, *251*(2), Article 51. https://doi.org/10.1007/s00425-020-03341-1

Dobrotvorskiy, D., Dobrotvorskaya, T., & Martynov, S. (2023). *GRIS: Genetic resources information system for wheat and triticale*. http://wheatpedigree.net

Ellis, M., Spielmeyer, W., Gale, K., Rebetzke, G., & Richards, R. (2002). "Perfect" markers for the *Rht-B1b* and *Rht-D1b* dwarfing genes in wheat. *Theoretical and Applied Genetics*, *105*, 1038–1042. https://doi.org/10.1007/s00122-002-1048-4

Emebiri, L. C., Oliver, J. R., Mrva, K., & Mares, D. (2010). Association mapping of late maturity α-amylase (LMA) activity in a collection of synthetic hexaploid wheat. *Molecular Breeding*, *26*(1), 39–49. https://doi.org/10.1007/s11032-009-9375-7

Fairlie, W., Edwards, J., Mather, D., & Kuchel, H. (2022). End-use quality of wheat affected by late maturity α-amylase. *Journal of Cereal Science*, *109*, 103610. https://doi.org/10.1016/j.jcs.2022.103610

Fairlie, W., Norman, A., Edwards, J., Mather, D. E., & Kuchel, H. (2024). Genetic analysis of late-maturity alpha-amylase in twelve wheat populations. *Planta*, *259*(2), Article 40. https://doi.org/10.1007/s00425-023-04319-5

Farrell, A. D., Kettlewell, P. S., Simmonds, J., Flintham, J. E., Snape, J. W., Werner, P., & Jack, P. L. (2013). Control of late maturity alpha-amylase in wheat by dwarfing gene *Rht-D1b* and genes on the 1B/1R translocation. *Molecular Breeding*, *32*(2), 425–436. https://doi.org/10.1007/s11032-013-9881-5

Fu, B. X., Hatcher, D. W., & Schlichting, L. (2014). Effects of sprout damage on durum wheat milling and pasta processing quality. *Canadian Journal of Plant Science*, *94*, 545–553. https://doi.org/10.4141/cjps2013-094

Gale, M. D., Flintham, J. E., & Arthur, E. D. (1983). Alpha-amylase production in the late stages of grain-development – an early sprouting damage risk period? In J. E. Kruger & D. E. LaBerge (Eds.), *Proceedings of the Third International Symposium on Preharvest Sprouting in Cereals* (pp. 29–35). Westview Press (Boulder, CO).

Gale, M. D., & Youssefian, S. (1975). Dwarfing genes in wheat. In G. E. Russel (Ed.), *Progress in plant breeding* (pp. 1–35). Buttersworth.

Gilmour, A. R., Thompson, R., & Cullis, B. R. (1995). Average information REML: An efficient algorithm for variance parameter estimation in linear mixed models. *Biometrics*, *51*(4), 1440–1450. https://doi.org/10.2307/2533274

Hagberg, S. (1960). A rapid method for determining alpha-amylase activity. *Cereal Chemistry*, *37*, 218–222.

Hagberg, S. (1961). Note on a simplified rapid method for determining α-amylase activity. *Cereal Chemistry*, *38*, 202–203.

Hauvermale, A. L., Ariizumi, T., & Steber, C. M. (2012). Gibberellin signaling: A theme and variations on DELLA repression. *Plant Physiology*, *160*, 83–92. https://doi.org/10.1104/pp.112.200956

Hauvermale, A. L., Parveen, R. S., Harris, T. J., Tuttle, K. M., Mikhaylenko, G., Nair, S., McCubbin, A. G., Pumphrey, M. O., & Steber, C. M. (2023). Streamlined α-amylase assays for wheat preharvest sprouting and late maturity α-amylase detection. *Agrosystems, Geosciences & Environment*, *6*(1), e20327. https://doi.org/10.1002/agg2.20327

Henderson, C. R. (1975). Best linear unbiased estimation and prediction under a selection model. *Biometrics*, *31*(2), 423–447. https://doi.org/10.2307/2529430

Hirano, K., Aya, K., Hobo, T., Sakakibara, H., Kojima, M., Shim, R. A., Hasegawa, Y., Ueguchi-Tanaka, M., & Matsuoka, M. (2008). Comprehensive transcriptome analysis of phytohormone biosynthesis and signaling genes in microspore/pollen and tapetum of rice. *Plant Cell Physiology*, *49*(10), 1429–1450. http://doi.org/10.1093/pcp/pcn123

Hu, Y., Sjoberg, S. M., Chen, C. J., Hauvermale, A. L., Morris, C. F., Delwiche, S. R., Cannon, A. E., Steber, C. M., & Zhang, Z. (2022). As the number falls, alternatives to the Hagberg–Perten falling number method: A review. *Comprehensive Reviews in Food Science and Food Safety*, *21*(3), 2105–2117. https://doi.org/10.1111/1541-4337.12959

International Wheat Genome Sequencing Consortium (IWGSC). (2018). Shifting the limits in wheat research and breeding using a fully annotated reference genome. *Science*, *361*(6403), eaar7191. https://doi.org/10.1126/science.aar7191

Jones, S. S., Lyon, S. R., Balow, K. A., Gollnick, M. A., Murphy, K. M., Kuehner, J. S., Murray, T. D., Chen, X. M., Engle, D. A., & Campbell, K. G. (2010). Registration of 'Xerpha' wheat. *Journal of Plant Registrations*, *4*(2), 137–140. https://doi.org/10.3198/jpr2009.06.0306crc

Kiszonas, A. M., Engle, D. A., Pierantoni, L. A., & Morris, C. F. (2018). Relationships between falling number, α-amylase activity, milling, cookie, and sponge cake quality of soft white wheat. *Cereal Chemistry*, *95*(3), 373–385. https://doi.org/10.1002/CCHE.10041

Kondhare, K. R., Farrell, A. D., Kettlewell, P. S., Hedden, P., & Monaghan, J. M. (2015). Pre-maturity alpha-amylase in wheat: The role of abscisic acid and gibberellins. *Journal of Cereal Science*, *63*, 95–108. https://doi.org/10.1016/j.jcs.2015.03.004

Kondhare, K. R., Kettlewell, P. S., Farrell, A. D., Hedden, P., & Monaghan, J. M. (2013). The role of sensitivity to abscisic acid and gibberellin in pre-maturity alpha-amylase formation in wheat grains. *Journal of Cereal Science*, *58*(3), 472–478. https://doi.org/10.1016/j.jcs.2013.09.009

Kosambi, D. D. (1943). The estimation of map distances from recombination values. *Annals of Eugenics*, *12*(1), 172–175. https://doi.org/10.1111/j.1469-1809.1943.tb02321.x

Kulwal, P. L., Singh, R., Balyan, H. S., & Gupta, P. K. (2004). Genetic basis of pre-harvest sprouting tolerance using single-locus and two-locus QTL analyses in bread wheat. *Functional and Integrative Genomics*, *4*, 94–101. https://doi.org/10.1007/s10142-004-0105-2

Kumar, S., Knox, R. E., Clarke, F. R., Pozniak, C. J., Depauw, R. M., Cuthbert, R. D., & Fox, S. (2015). Maximizing the identification of QTL for pre-harvest sprouting resistance using seed dormancy measures in a white-grained hexaploid wheat population. *Euphytica*, *205*, 287–309. https://doi.org/10.1007/s10681-015-1460-x

Liu, C., Parveen, R. S., Revolinksi, S. R., Garland-Campbell, K. A., Pumphrey, M. O., & Steber, C. M. (2021). The genetics of late maturity *α*-amylase (LMA) in North American spring wheat (*Triticum aestivum* L.). *Seed Science Research*, *31*, 159–168. https://doi.org/10.1017/S0960258521000064

Liu, C., Tuttle, K. M., Garland Campbell, K. A., Pumphrey, M. O., & Steber, C. M. (2021). Investigating conditions that induce late maturity *α*-amylase (LMA) using Northwestern US spring wheat (*Triticum aestivum* L.). *Seed Science Research*, *31*(3), 169–177. https://doi.org/10.1017/S0960258521000052

Mares, D., Derkx, A., Cheong, J., Zaharia, I., Asenstorfer, R., & Mrva, K. (2022). Gibberellins in developing wheat grains and their relationship to late maturity *α*-amylase (LMA). *Planta*, *255*(6), Article 119. https://doi.org/10.1007/s00425-022-03899-y

Mares, D., Derkx, A., Mather, D. E., Cheong, J., & Mrva, K. (2023). Multiple loci with cumulative effects on late maturity *α*-amylase (LMA) in wheat. *Planta*, *257*(5), Article 96. https://doi.org/10.1007/s00425-023-04131-1

Mares, D., Derkx, A., & Mrva, K. (2024). Late maturity alpha-amylase (LMA) in gibberellin-insensitive, semi-dwarf wheat (*Triticum aestivum* L.). *Journal of Cereal Science*, *116*, 103858. https://doi.org/10.1016/j.jcs.2024.103858

Mares, D., & Mrva, K. (2008). Late-maturity *α*-amylase: Low falling number in wheat in the absence of preharvest sprouting. *Journal of Cereal Science*, *47*(1), 6–17. https://doi.org/10.1016/j.jcs.2007.01.005

Mares, D. J., & Gale, M. D. (1990). Control of alpha-amylase synthesis in wheat. In K. Ringlund, E. Mosleth, & D. J. Mares (Eds.), *Proceedings of the Fifth International Symposium on Pre-Harvest Sprouting in Cereals* (pp. 167–175). Westview Press (Boulder, CO).

Mares, D. J., & Mrva, K. (1993). Late maturity alpha-amylase synthesis in wheat. In M. K. Walker-Simmons, & J. L. Reid (Eds.), *Fifth international symposium on pre-harvest sprouting in cereals* (pp. 183–194). Westview Press.

Mares, D. J., & Mrva, K. (2014). Wheat grain preharvest sprouting and late maturity *α*-amylase. *Planta*, *240*(6), 1167–1178. https://doi.org/10.1007/s00425-014-2172-5

Martinez, S. A., Tuttle, K. M., Takebayashi, Y., Seo, M., Campbell, K. G., & Steber, C. M. (2016). The wheat ABA hypersensitive *ERA8* mutant is associated with increased preharvest sprouting tolerance and altered hormone accumulation. *Euphytica*, *212*, 229–245. https://doi.org/10.1007/s10681-016-1763-6

McGinnis, K. M., Thomas, S. G., Soule, J. D., Strader, L. C., Zale, J. M., Sun, T., & Steber, C. M. (2003). The Arabidopsis *SLEEPY1* gene encodes a putative F-box subunit of an SCF E3 ubiquitin ligase. *The Plant Cell*, *15*(5), 1120–1130. https://doi.org/10.1105/tpc.010827

McNeil, M. D., Diepeveen, D., Wilson, R., Barclay, I., McLean, R., Chalhoub, B., & Appels, R. (2009). Haplotype analyses in wheat for complex traits: Tracking the chromosome 3B and 7B regions associated with late maturity alpha amylase (LMA) in breeding programs. *Crop Pasture Science*, *60*(5), 463–471. https://doi.org/10.1071/CP08340

Mieog, J. C., Janeček, Š., & Ral, J. P. (2017). New insight in cereal starch degradation: Identification and structural characterization of four *α*-amylases in bread wheat. *Amylase*, *1*(1), 35–49. https://doi.org/10.1515/amylase-2017-0004

Mohan, A., Kulwal, P., Singh, R., Kumar, V., Mir, R. R., Kumar, J., Prasad, M., Balyan, H. S., & Gupta, P. K. (2009). Genome-wide QTL analysis for pre-harvest sprouting tolerance in bread wheat. *Euphytica*, *168*, 319–329. https://doi.org/10.1007/s10681-009-9935-2

Mohler, V., Albrecht, T., Mrva, K., Schweizer, G., & Hartl, L. (2014). Genetic analysis of falling number in three bi-parental common winter wheat populations. *Plant Breeding*, *133*(4), 448–453. https://doi.org/10.1111/pbr.12177

Money, D., Gardner, K., Migicovsky, Z., Schwaninger, H., Zhong, G. Y., & Myles, S. (2015). LinkImpute: Fast and accurate genotype imputation for nonmodel organisms. *G3 Genes|Genomes|Genetics*, *5*(11), 2383–2390. https://doi.org/10.1534/g3.115.021667

Mrva, K., Cheong, J., Yu, B., Law, H. Y., & Mares, D. (2009). Late maturity *α*-amylase in synthetic hexaploid wheat. *Euphytica*, *168*(3), 403–411. https://doi.org/10.1007/s10681-009-9931-6

Mrva, K., & Mares, D. (1996a). Control of later maturity *α*-amylase synthesis compared to enzyme synthesis during germination. In K. Noda & D. J. Mares (Eds.), *Proceedings of the Seventh International Symposium on Pre-Harvest Sprouting in Cereals* (pp. 419–426). Westview Press (Osaka, Japan).

Mrva, K., & Mares, D. J. (1996b). Expression of late maturity *α*-amylase in wheat containing gibberellic acid insensitivity genes. *Euphytica*, *88*(1), 69–76. https://doi.org/10.1007/BF00029267

Mrva, K., & Mares, D. J. (2001a). Induction of late maturity a-amylase in wheat by cool temperature. *Crop and Pasture Science*, *52*, 477–484. https://doi.org/10.1071/AR00097

Mrva, K., & Mares, D. J. (2001b). Quantitative trait locus analysis of late maturity *α*-amylase in wheat using doubled haploid population Cranbrook × Halberd. *Crop and Pasture Science*, *52*, 1267–1273. https://doi.org/10.1071/AR01047

Mrva, K., & Mares, D. J. (2001c). Relationship between black point, late maturity alpha-amylase, and sprouting tolerance in wheat. In M. Wooton, I. L. Batey, & C. W. Wrigley (Eds.), In *Proceedings of the 11th ICC cereal and bread congress and of the 50th Australian cereal chemistry conference* (pp. 249–252). RACI Cereal Chemistry Division.

Mrva, K., Wallwork, M., & Mares, D. J. (2006). *α*-Amylase and programmed cell death in aleurone of ripening wheat grains. *Journal of Experimental Botany*, *57*(4), 877–885. https://doi.org/10.1093/jxb/erj072

Neoh, G. K. S., Dieters, M. J., Tao, K., Fox, G. P., Nguyen, P. T. M., & Gilbert, R. G. (2021). Late-maturity *α*-amylase in wheat (*Triticum* *aestivum*) and its impact on fresh white sauce qualities. *Foods*, *10*(2), 201. https://doi.org/10.3390/foods10020201

Newberry, M., Zwart, A. B., Whan, A., Mieog, J. C., Sun, M., Leyne, E., Pritchard, J., Daneri-Castro, S. N., Ibrahim, K., Diepeveen, D., Howitt, C. A., & Ral, J.-P. F. (2018). Does late maturity α-amylase impact wheat baking quality? *Frontiers in Plant Science*, *9*, Article 1356. https://doi.org/10.3389/fpls.2018.01356

North Carolina State University, Bioinformatics Research Center. (2010). *Windows QTL cartographer 2.5 user manual*. NC State University. https://brcwebportal.cos.ncsu.edu/qtlcart/WinQTLCart.pdf

Olaerts, H., & Courtin, C. M. (2018). Impact of preharvest sprouting on endogenous hydrolases and technological quality of wheat and bread: A review. *Comprehensive Reviews in Food Science and Food Safety*, *17*(3), 698–713. https://doi.org/10.1111/1541-4337.12347

Ouellette, L. A., Reid, R. W., Blanchard, S. G., & Brouwer, C. R. (2018). LinkageMapView—Rendering high-resolution linkage and QTL maps. *Bioinformatics*, *34*(2), 306–307. https://doi.org/10.1093/bioinformatics/btx576

Pearce, S., Saville, R., Vaughan, S. P., Chandler, P. M., Wilhelm, E. P., Sparks, C. A., Al-Kaff, N., Korolev, A., Boulton, M. I., Phillips, A. L., Hedden, P., Nicholson, P., & Thomas, S. G. (2011). Molecular characterization of *Rht*-1 dwarfing genes in hexaploid wheat. *Plant Physiology*, *157*, 1820–1831. https://doi.org/10.1104/pp.111.183657

Peery, S. R., Carle, S. W., Wysock, M., Pumphrey, M. O., & Steber, C. M. (2023). LMA or vivipary? Wheat grain can germinate precociously during gran maturation under the cool conditions used to induce late maturity alpha-amylase (LMA). *Frontiers in Plant Science*, *14*, 1156784. https://doi.org/10.3389/fpls.2023.1156784

Peng, J., Richards, D. E., Hartley, N. M., Murphy, G. P., Devos, K. M., Flintham, J. E., Beales, J., Fish, L. J., Worland, A. J., Pelica, F., Sudhakar, D., Christou, P., Snape, J. W., Gale, M. D., & Harberd, N. P. (1999). "Green revolution" genes encode mutant gibberellin response modulators. *Nature*, *400*, 256–261. https://doi.org/10.1038/22307

Pereira, M. J., Pfahler, P. L., Barnett, R. D., Blount, A. R., Wofford, D. S., & Littell, R. C. (2002). Coleoptile length in dwarf wheat isolines. *Crop Science*, *42*, 1483–1487. https://doi.org/10.2135/cropsci2002.1483

Perten, H. (1964). Application of the falling number method for evaluating α-amylase activity. *Cereal Chemistry*, *41*(3), 127–139.

Poland, J. A., Brown, P. J., Sorrells, M. E., & Jannink, J. L. (2012). Development of high-density genetic maps for barley and wheat using a novel two-enzyme genotyping-by-sequencing approach. *PLoS ONE*, *7*(2), e32253. https://doi.org/10.1371/journal.pone.0032253

Qi, W., Sun, F., Wang, Q., Chen, M., Huang, Y., Feng, Y.-Q., Luo, X., & Yang, J. (2011). Rice ethylene—Response AP2/ERF factor *OsEATB* restricts internode elongation by down-regulation gibberellin biosynthetic gene. *Plant Physiology*, *157*(1), 216–228. https://doi.org/10.1104/pp.111.179945

Ral, J.-P. F., Sun, M., Mathy, A., Pritchard, J. R., Konik-Rose, C., Larroque, O., & Newberry, M. (2018). A biotechnological approach to directly assess the impact of elevated endogenous α-amylase on Asian white-salted noodle quality. *Starch*, *70*(1–2), 1700089. https://doi.org/10.1002/star.201700089

Rasul, F., Muhammad, R., Vakhtang, S., Hill, S., Islam, A., Iosiliani, O., & Loyd, N. (2015, July 1). *Agricultural weather network (AgWeatherNet): Science for society* [Paper presentation]. 2015 Science at IAREC, Prosser, WA.

Ross, A. S., & Bettge, A. (2009). Passing the test on wheat end-use quality. In B. F. Carver (Ed.), *Wheat: Science and trade* (pp. 455–494). US Department of Agriculture. https://doi.org/10.1002/9780813818832

Ross, A. S., Flowers, M. D., Zemetra, R. S., & Kongraksawech, T. (2012). Effect of grain protein concentration on falling number of ungerminated soft white winter wheat. *Cereal Chemistry*, *89*(6), 307–310. https://doi.org/10.1094/CCHEM-07-12-0085-RC

Schuelke, M. (2000). An economic method for the fluorescent labeling of PCR fragments. *Nature Biotechnology*, *18*(2), 233–234. https://doi.org/10.1038/72708

Shalmani, A., Huang, Y. B., Chen, Y. B., Muhammad, I., Li, B. B., Ullah, U., Jing, X. Q., Bhanbhro, N., Liu, W. T., Li, W. Q., & Chen, K. M. (2021). The highly interactive BTB domain targeting other functional domains to diversify the function of BTB proteins in rice growth and development. *International Journal of Biological Macromolecules*, *192*, 1311–1324. https://doi.org/10.1016/j.ijbiomac.2021.10.046

Sjoberg, S. M., Carter, A. H., Steber, C. M., & Garland Campbell, K. A. (2020). Application of the factor analytic model to assess wheat falling number performance and stability in multi-environment trials. *Crop Science*, *61*(1), 372–382. https://doi.org/10.1002/csc2.20293

Somers, D. J., Isaac, P., & Edwards, K. (2004). A high-density microsatellite consensus map for bread wheat (*Triticum aestivum* L.). *Theoretical and Applied Genetics*, *109*(6), 1105–1114. https://doi.org/10.1007/s00122-004-1740-7

Steber, C. M. (2022). *Rising to the challenge of falling numbers*. Washington Grains. https://wagrains.org/articles/rising-to-the-challenge-of-falling-numbers/

Steber, C. M., Pumphrey, M. O., & Carter, A. H. (2018). Hunting for genes. *Wheat Life*, *61*, 50–51.

Tan, M. K., Verbyla, A. P., Cullis, B. R., Martin, P., Milgate, A. W., & Oliver, J. R. (2010). Genetics of late maturity α-amylase in a doubled haploid wheat population. *Crop Pasture Science*, *61*(2), 153–161. https://doi.org/10.1071/CP09239

Tuttle, K. M., Martinez, S. A., Schramm, E. C., Takebayashi, Y., Seo, M., & Steber, C. M. (2015). Grain dormancy loss is associated with changes in ABA and GA sensitivity and hormone accumulation in bread wheat, *Triticum aestivum* (L.). *Seed Science Research*, *25*(2), 179–193. https://doi.org/10.1017/S0960258515000057

Van Ooijen, J. W., Ooijen, J. W., Verlaat, J. V., Ooijen, J. W., Tol, J., Dalén, J., Buren, J. B., Meer, J. V., Krieken, J. H., Ooijen, J. W., Kessel, J. S., Van, O., Voorrips, R. E., & Heuvel, L. P. (2006). *JoinMap® 4, software for the calculation of genetic linkage maps in experimental populations*. Kyazma B.V.

Verbyla, A. P., & Cullis, B. R. (2012). Multivariate whole genome average interval mapping: QTL analysis for multiple traits and/or environments. *Theoretical and Applied Genetics*, *125*(5), 933–953. https://doi.org/10.1007/s00122-012-1884-9

Wang, S., Wong, D., Forrest, K., Allen, A., Chao, S., Huang, B. E., Maccaferri, M., Salvi, S., Milner, S. G., Cattivelli, L., Mastrangelo, A. M., Whan, A., Stephen, S., Barker, G., Wieseke, R., Plieske, J., Lillemo, M., Mather, D., Appels, R., … Akhunov, E. (2014). Characterization of polyploid wheat genomic diversity using a high-density 90,000 single nucleotide polymorphism array. *Plant Biotechnology Journal*, *12*(6), 787–796. https://doi.org/10.1111/pbi.12183

Xu, Q., Truong, T. T., Barrero, J. M., Jacobsen, J. V., Hocart, C. H., & Gubler, F. (2016). A role for jasmonates in the release of dormancy by cold stratification in wheat. *Journal of Experimental Botany*, *67*(11), 3497–3508. https://doi.org/10.1093/jxb/erw172

Yamauchi, Y., Ogawa, M., Kuwahara, A., Hanada, A., Kamiya, Y., & Yamaguchi, S. (2004). Activation of gibberellin biosynthesis and response pathways by low temperature during imbibition of *Arabidopsis thaliana* seeds. *The Plant Cell*, *16*(2), 367–378. https://doi.org/10.1105/tpc.018143

Yates, A. D., Allen, J., Amode, R. M., Azov, A. G., Barba, M., Becerra, A., Bhai, J., Campbell, L. I., Carbajo Martinez, M., Chakiachvili, M., Chougule, K., Christensen, M., Contreras-Moreira, B., Cuzick, A., Da Rin Fioretto, L., Davis, P., De Silva, N. H., Diamantakis, S., Dyer, S., … Flicek, P. (2022). Ensembl genomes 2022: An expanding genome resource for non-vertebrates. *Nucleic Acids Research*, *50*(D1), D996–D1003. https://doi.org/10.1093/nar/gkab1007

Youssefian, S., Kirby, E. J. M., & Gale, M. D. (1992). Pleiotropic effects of the GA-insensitive *Rht* dwarfing genes in wheat. 2. Effects on leaf, stem, ear, and floret growth. *Field Crops Research*, *28*, 191–210. https://doi.org/10.1016/0378-4290(92)90040-G

Zadoks, J. C., Chang, T. T., & Konzak, C. F. (1974). A decimal code for the growth stages of cereals. *Weed Research*, *14*(6), 415–421. https://doi.org/10.1111/j.1365-3180.1974.tb01084.x

Zemetra, R. S., Larson, M., Heesacker, A., Simons, E., Flowers, M., Haggard, K., Ross, A., Ong, C., Mundt, C., Chen, X., & Morris, C. (2013). *Proposal for release of OR08047P94 'Bobtail' soft white winter wheat*. Oregon Agricultural Experiment Station.

Zeng, M., Morris, C. F., Batey, I. L., & Wrigley, C. W. (1997). Sources of variation for starch gelatinization, pasting, and gelation properties in wheat. *Cereal Chemistry*, *74*(1), 63–71. https://doi.org/10.1094/CCHEM.1997.74.1.63

Zhang, J., Chen, J., Bowman, B. C., O'brien, K., Marshall, J. M., & Bonman, J. M. (2014). Association mapping of Hagberg falling number in hard white spring wheat. *Crop Science*, *54*(3), 1243–1252. https://doi.org/10.2135/cropsci2013.08.0551

Zhang, Y., Liu, H., & Yan, G. (2021). Characterization of near-isogenic lines confirmed QTL and revealed candidate genes for plant height and yield-related traits in common wheat. *Molecular Breeding*, *41*(1), Article 4. https://doi.org/10.1007/s11032-020-01196-8

Zhu, W. (2022). Genome-wide identification and analysis of analysis of BURP genes in *Triticum aestivum*. *BioRxiv*. https://doi.org/10.1101/2022.10.21.513156

Zuo, J., Lin, C. T., Cao, H., Chen, F., Liu, Y., & Liu, J. (2019). Genome-wide association study and quantitative trait loci mapping of seed dormancy in common wheat (*Triticum aestivum* L.). *Planta*, *250*, 187–198. https://doi.org/10.1007/s00425-019-03164-9

SUPPORTING INFORMATION

Additional supporting information can be found online in the Supporting Information section at the end of this article.

How to cite this article: Marston, E. J., Hooker, M. A., Marlowe, K., Ruff, T. R., Liu, Y., Carle, S. W., Parveen, R. S., Trittinger, S., See, D. R., & Steber, C. M. (2025). Identification of LMA-tolerance QTL in a biparental winter wheat mapping population (Xerpha/Bobtail). *Crop Science*, *65*, e70089. https://doi.org/10.1002/csc2.70089